*Aust. J. Phys.*, 1980, **33**, 639–69

# Survey of OH Masers at 1665 and 1667 MHz. I Galactic Longitudes 326° to 340°

*J. L. Caswell,*[A] *R. F. Haynes*[A] *and W. M. Goss*[B]

[A] Division of Radiophysics, CSIRO, P.O. Box 76, Epping, N.S.W. 2121.
[B] Kapteyn Astronomical Institute, University of Groningen, Postbus 800, Groningen, Netherlands.

*Abstract*

The galactic plane between longitudes 326° and 340° has been searched for OH emission and absorption on the 1665 and 1667 MHz transitions. Forty main-line emission sources were detected (27 new ones, 13 previously known), and these constitute a sample complete to a well-defined lower intensity limit in this region of sky. Line profiles of all sources are shown and the statistics on variability and on the intensity ratios of the ground state transitions are summarized. The completeness of the sample encouraged us to make a first attempt to construct a luminosity function and to estimate the total number of such masers in our Galaxy. A study of the velocity structures showed these to be extremely varied, but none exceed a total range of 25 km s$^{-1}$; combined velocity and polarization data are compatible with a Zeeman splitting origin for the circular polarization, and with this interpretation several sources yield an estimate for the line-of-sight magnetic field strength of a few mG. Preliminary investigations of the associations with other celestial objects indicate that many of the masers are loosely associated with HII region complexes, but in at least eight instances no HII regions have yet been detected; of these eight masers, two may be associated with supernova remnants and one with an unidentified nonthermal radio source.

## 1. Introduction

Most searches for OH line radiation on the 1665 and 1667 MHz transitions have been made at the positions of other objects of interest, e.g. HII regions, dust clouds and various types of stars. However, it is clearly desirable to make unbiased OH searches in order to obtain a clearer guide to the frequency of occurrence of different classes of OH source; a small survey of this kind, resulting in the detection of four OH masers, was conducted by Elldér *et al.* (1969). The search reported here, conducted along the galactic plane between longitudes 326° and 340°, detected 40 OH masers. This main-line search complements our earlier satellite-line searches over the same region (Caswell and Haynes 1975, hereafter referred to as CH; Haynes and Caswell 1977, hereafter HC), and these earlier surveys facilitated the classification of the new sources. We propose to make similar surveys of other portions of the Galaxy.

## 2. Observations

The procedures and equipment were generally similar to the 1612 and 1720 MHz surveys (CH; HC) but with several improvements to the receiver system. All observations were made with a dual channel 18 cm parametric amplifier installed on the Parkes 64 m paraboloid; the system temperature of each channel was $\sim$80 K on cold regions of sky. Two orthogonal linear polarizations were sampled and with appropriate phasing were combined at IF to yield the two senses (RH and LH) of circular polarization. The spectral line analysis was performed with the 1024 channel digital autocorrelator, yielding a 512 point spectrum for each circular polarization simultaneously.

The intensity calibration is relative to Hydra A, for which a total flux density of 36 Jy was assumed (18 Jy in each sense of circular polarization; note that with this convention, the total flux density is the sum of the intensities in the two circular polarizations, not the mean, the ratio of flux density to antenna temperature for *each* polarization being $0 \cdot 8$ Jy $K^{-1}$). The beamwidth to half-power is 12′ arc at 1666 MHz.

*The Searches*: *1975 June 18–23 and 1976 February 25 to March 5*

Observations in the first period were made on the 1667 MHz transition and in the second on the 1665 MHz transition. Both searches covered a grid at $b = 0°$ and $\pm 0° \cdot 2$, spaced $0° \cdot 2$ in longitude between 326° and 340°. Positions with $|b| = 0° \cdot 4$ and larger were also observed when OH emission was detected at the edge of the original grid or where the continuum emission (see e.g. Haynes *et al.* 1978) extends significantly outside the $\pm 0° \cdot 3$ region. The spectrum bandwidth analysed was 1 MHz wide and covered the radial velocity range $-160$ to $+20$ km $s^{-1}$ (l.s.r.). The resolution (with uniform weighting) was $2 \cdot 4$ kHz ($\equiv 0 \cdot 4$ km $s^{-1}$). Seven-minute integrations at each grid position, combined with a 15 min reference, yielded an r.m.s. noise level of $\sim 0 \cdot 15$ K ($\equiv 0 \cdot 12$ Jy in each sense of polarization) in directions with no strong continuum radio sources.

*Further Study*: *1975 August 1–6*; *1976 July 14–19*; *1978 August 16–24*

In the first two sessions an accurate position was measured for each source using a grid with 6′ arc spacing centred on the approximate source position. Observations were then made at the source position with higher frequency resolution (usually a $0 \cdot 2$ MHz total bandwidth was used yielding a resolution of $0 \cdot 8$ kHz $\equiv 0 \cdot 14$ km $s^{-1}$). In the most recent session a complete set of profiles of all detected OH sources was obtained to assess the variability over a period of two or more years.

## 3. Results

### (*a*) *OH Emission—Tabulation and Figures*

In Table 1 we list the main-line emission sources located in the survey region. These are OH masers emitting at either 1665 or 1667 MHz but excluding three OH/IR stars (discovered by CH) in which main-line emission accompanies stronger 1612 MHz emission. These OH/IR stars are: OH/IR $327 \cdot 1-0 \cdot 3$ (weak 1667 MHz emission at $V \approx -90$ km $s^{-1}$); OH/IR $328 \cdot 2+0 \cdot 0$ (weak 1667 MHz emission at $V = -30$ to $-40$ km $s^{-1}$ and $-75$ to $-82$ km $s^{-1}$); and OH/IR $337 \cdot 9+0 \cdot 3$, which is somewhat unusual since it shows 1612 MHz emission near $V = -78$ and $-39$ km $s^{-1}$ and emission of comparable intensity at 1667 MHz extending from $-90$ to $-60$ km $s^{-1}$. Most of those in the direction of strong HII regions had been found in previous searches (Goss *et al.* 1970, hereafter referred to as GMR; Robinson *et al.* 1974, hereafter RCG) and several others were found by accident in the follow-up to our 1612 MHz survey (CH). For the source name we use the prefix OH followed by the galactic coordinates, *l* and *b*, rounded to the nearest $0 \cdot 01$ degree (quoting them to lesser accuracy can lead to ambiguities, and future position refinements should not cause changes exceeding one in the last (rounded) digit).

Details of each source are best displayed in the figures, but Table 1 provides a brief summary, including the range of radial velocity over which emission is detectable and the intensity and polarization of the peak of emission. At 1665 and 1667 MHz the latter measurements are for August 1978; at 1612 MHz the data are inhomogeneous with respect to epoch and spectral resolution. Emission at 1612 MHz referred to as 'weak' is probably of type IIc (see CH) and not closely related to the main-line maser emission. At 1720 MHz no emission related to the main-line masers of Table 1 has been found. For some sources which show emission on several transitions the position has been accurately measured on all transitions and an average is quoted; in other cases the accurate measurement has been made only on one transition (as indicated) while the position estimates for the other transitions are cruder but compatible with being coincident. Where a source was discovered in earlier work a reference is given (column 10) but it is enclosed in parentheses if no previous profile has been published. The presence or absence of an $H_2O$ maser or a maser on the most common of the excited OH transitions (6035 MHz line in the $^2\pi_{3/2}\, J = 5/2$ state) is noted by a Y (yes) or N (no); detections which are doubtful or perhaps displaced in position are accompanied by a question mark (see Batchelor *et al.* 1979 for $H_2O$ data and Knowles *et al.* 1976 for OH data). Any continuum source in the same direction is noted in column 13 (see the map of Haynes *et al.* 1978). The kinematic distance to the maser is quoted in column 14 and is based on the Schmidt (1965) galactic rotation model; in this region of the Galaxy there is a distance ambiguity, but in cases where an HII region appears to be associated and its distance ambiguity has been resolved (Caswell *et al.* 1975) this preferred distance is given in italics.

A profile of each source is shown in Figs 1–17: the 1665 MHz profile is shown in every case, whereas at 1667 MHz a profile was observed in every case but is not shown where no emission was detected (the noise level being similar to that of the 1665 MHz profile). For one source (OH 327·29−0·58 in Fig. 2), profiles at two dates are shown to demonstrate variability with time; all the other profiles were taken in August 1978. In several instances two sources are separated by less than the telescope beamwidth and so when pointing at one source the other is weakly detectable; in these confused cases the weaker offset source is indicated and labelled with its name in parentheses. The large scale in intensity was chosen to make weak features readily visible; this scale necessitated truncation of some strong single features, and peak intensities are labelled in such cases.

### (*b*) *Notes on Some Individual OH Sources*

In these notes we draw attention to any unusual properties and give additional comments on the following.

(1) Any intensity variations from July 1976 to August 1978; in the absence of any comment the variability is $<20\%$.
(2) The presence of 1612 MHz emission when it occurs.
(3) Pairs of right and left circular components which are suggestive of the pattern arising from Zeeman splitting in a magnetic field.
(4) Some unusual apparent associations with continuum radio sources, in particular, with two supernova remnants (SNRs).
(5) Closely spaced OH sources where some danger of confusion exists.

**Table 1. OH main-line masers in survey region** 326° < $l$ < 340°

Listed here are OH masers emitting at either 1665 or 1667 MHz but excluding OH/IR stars with weak emission accompanying much stronger 1612 MHz emission (see text)

| (1) Galactic coordinates $l$ ° | (2) $b$ ° | (3) Position (1950) R.A. h m s | (4) Dec. ° ′ ″ | (5) r.m.s. error ″ | (6) Radial velocity[A] (l.s.r.) (km s$^{-1}$) | (7) Intensity (poln) of peak[B] 1665 (Jy) | (8) 1667 (Jy) | (9) 1612 (Jy) | (10) OH Refs[C] | (11) Excited OH? | (12) $H_2O$? | (13) Radio continuum | (14) Kinematic distance[D] (kpc) |
|---|---|---|---|---|---|---|---|---|---|---|---|---|---|
| 326·77 | −0·26 | 15 45 04·1 | −54 32 40 | 60 | −58 | *2·5*(L) | — | — | | | (N) | Weak extended | 4·0, 12·6 |
| 327·12 | +0·51 | 15 43 41·8 | −53 43 23 | 18 | −88, −80 | *7·6*(L) | *2·4*(L) | — | | | Y | Weak | 6·1, 10·8 |
| 327·29 | −0·58 | 15 49 12·8 | −54 28 29 | 35 | −72, −54 | *22*(R) | 1·1(R) | — | RCG | N | Y | Strong HII | *4·4*, (12·4) |
| 327·40 | +0·45 | 15 45 28·5 | −53 36 09 | 18 | −83, −76 | *8·0*(R) | 1·1(L) | — | | | Y | SNR (see text) | 5·6, 11·3 |
| 328·24 | −0·54 | 15 54 04·9 | −53 50 09 | 24 | −47, −35 | *9·6*(R) | 3·2(L) | — | RCG | N | N | Edge HII | 2·9, 14·1 |
| 328·30 | +0·44 | 15 50 13·7 | −53 02 52 | 16 | −94, −90 | *19·0*(L) | 0·6(L) | Weak | | | Y | HII | 6·9, 10·2 |
| 328·81 | +0·64 | 15 51 59·0 | −52 34 24 | 15 | −49, −36 | *129*(R) | 12·8(R) | 6·5(R) | | | N | Compact source | 3·1, 14·0 |
| 329·04 | −0·21 | 15 56 43·8 | −53 04 11 | 15 | −46, −38 | *17·3*(L) | *2·9*(L) | Weak | (CH) | N | N | None? | 3·0, 14·1 |
| 329·18 | −0·32 | 15 57 56·3 | −53 03 27 | 15 | −56, −43 | *8·6*(R) | *4·1*(L) | — | (CH) | | Y | None? | 3·6, 13·6 |
| 329·40 | −0·46 | 15 59 41·1 | −53 01 33 | 16 | −76, −66 | *19*(L) | 8·5(R) | — | (CH) | N | Y | Very weak | 5·0, 12·2 |
| 330·89 | −0·36 | 16 06 29·8 | −51 57 38 | 20 | −72, −58 | *265*(L) | 93(L) | Weak | RCG | N | Y | HII | *4·6*, (12·8) |
| 330·96 | −0·18 | 16 06 05·0 | −51 47 02 | 16 | −102, −80 | *33*(R) | 23(L) | Weak | RCG | Y | Y | Edge HII | 6·7, 10·8 |
| 331·13 | −0·24 | 16 07 10·6 | −51 42 33 | 16 | −96, −88 | *16·8*(R) | 0·6(L) | — | | | Y | Edge HII | 6·8, 10·7 |
| 331·28 | −0·20 | 16 07 42·4 | −51 34 33 | 28 | −95, −79 | 5·8(R) | *2·1*(R) | — | | | N | HII | 6·3, 11·2 |
| 331·34 | −0·34 | 16 08 35·8 | −51 38 16 | 29 | −68, −66 | *5·4*(L) | 2·0(L) | — | RCG | N | N | HII | *4·8*, (12·8) |
| 331·52 | −0·10 | 16 08 23·2 | −51 20 45 | 16 | −102, −82 | 44(R) | 32(R) | *270*(R) | GMR | Y? | Y | Strong HII | *6·8*, (10·8) |
| 332·72 | −0·62 | 16 16 14·6 | −50 53 38 | 45 | −53, −45 | *1·2*(R) | 2·7(R) | | CHG | | Y? | Near HII | 3·7, 14·1 |
| 333·14 | −0·43 | 16 17 16·7 | −50 27 45 | 17 | −59, −44 | *31*(L) | 6(R) | — | GMR | Y | Y | HII | *3·8*, (14·0) |
| 333·24 | −0·06 | 16 16 06·1 | −50 07 58 | 15 | −92, −83 | 2·*3*(R) | — | ~*5*(L) | (CH) | | Y | Edge HII | 6·5, 11·4 |
| 333·45 | −0·18 | 16 17 32·3 | −50 04 08 | 60 | −50, −36 | *3·2*(R) | — | — | | | (N) | Edge strong HII | 3·3, 14·6 |
| 333·61 | −0·22 | 16 18 27·4 | −49 59 03 | 15 | −57, −46 | *9·0*(L) | 4·6(R) | *11*(R) | GMR | Y? | Y | Strong HII | *3·8*, (14·1) |
| 335·61 | −0·31 | 16 27 27·8 | −48 37 03 | 21 | −54, −49 | *2·8*(R) | — | — | | | N | Near HII | 4·1, 14·2 |
| 335·79 | +0·17 | 16 26 07·2 | −48 09 44 | 18 | −55, −51 | 0·6(R) | *3·5*(L) | — | | | Y | Near weak HII | 4·1, 14·1 |
| 336·36 | −0·15 | 16 29 50·9 | −47 57 46 | 32 | −83, −81 | *1·0*(R) | — | — | | | N? | HII complex | 6·3, 12·1 |
| 336·83 | +0·02 | 16 31 00·1 | −47 30 20 | 21 | −91, −73 | *2·0*(R) | — | — | | | N | HII | 6·3, 12·1 |
| 337·00 | −0·02 | 16 31 50·6 | −47 24 29 | 20 | −124, −120 | *2·8*(R) | — | — | | | Y | SNR (see text) | *9·2* |

**Table 1** (*Continued*)

| (1) | (2) | (3) | (4) | (5) | (6) | (7) | (8) | (9) | (10) | (11) | (12) | (13) | (14) |
|---|---|---|---|---|---|---|---|---|---|---|---|---|---|
| Galactic coordinates | | Position (1950) | | r.m.s. error | Radial velocity[A] (l.s.r.) | Intensity (poln) of peak[B] | | | OH Refs[C] | Excited OH? | $H_2O$? | Radio continuum | Kinematic distance[D] (kpc) |
| *l* | *b* | R.A. | Dec. | | | 1665 | 1667 | 1612 | | | | | |
| ° | ° | h m s | ° ′ ″ | ″ | (km s$^{-1}$) | (Jy) | (Jy) | (Jy) | | | | | |
| 337·40 | −0·41 | 16 35 09·9 | −47 22 22 | 15 | −58, −33 | *66*(R) | *45*(R) | — | | | Y | NT source (see text) | 3·7, 14·7 |
| 337·61 | −0·07 | 16 34 29·6 | −46 59 19 | 25 | −43, −39 | *2·5*(L) | — | — | | | | HII | 3·5, 15·0 |
| 337·71 | −0·06 | 16 34 49·8 | −46 54 48 | 17 | −55, −48 | *19*(L) | 6(L) | — | RCG | Y? | Y | HII | 4·2, 14·3 |
| 337·92 | −0·48 | 16 37 29·7 | −47 02 12 | 15 | −54, −32 | *9·1*(R) | *5·3*(L) | — | RCG | N | Y | HII | *3·6*, (14·9) |
| 338·00 | +0·14 | 16 35 09·1 | −46 34 03 | 15 | −41, −33 | *8·6*(L) | *13·3*(L) | Weak | | | Y | Diffuse HII | 3·2, 15·4 |
| 338·08 | +0·02 | 16 35 58·8 | −46 34 54 | 33 | −60, −46 | *2·2*(L) | — | — | | | N | Edge weak HII | 4·4, 14·2 |
| 338·28 | +0·54 | 16 34 32·1 | −46 05 02 | 25 | −64, −61 | *4·4*(L) | — | — | | | | None? | 5·0, 13·6 |
| 338·46 | −0·25 | 16 38 36·5 | −46 28 37 | 18 | −61, −55 | *5·1*(L) | 1·8(L) | — | | | N | Edge weak HII | 4·7, 13·9 |
| 338·47 | +0·29 | 16 36 20·3 | −46 06 47 | 17 | −34, −31 | *4·1*(L) | — | — | | | N | Edge extended HII | 2·9, 15·8 |
| 338·68 | −0·08 | 16 38 44·2 | −46 12 09 | 20 | −23, −20 | *2·0*(R,L) | — | — | | | N | Edge extended HII | 2·0, 16·6 |
| 338·88 | −0·08 | 16 39 29·4 | −46 03 05 | 29 | −39, −35 | *5·0*(L) | — | — | RCG | N | (N)? | HII | 3·3, 15·4 |
| 338·93 | +0·55 | 16 36 58·0 | −45 35 54 | 15 | −65, −57 | *38*(L) | 0·7(R) | *36*(R) | RCG | N | Y? | Edge HII | 5·0, 13·6 |
| 339·62 | −0·13 | 16 42 29·8 | −45 31 43 | 15 | −41, −30 | *12·2*(R) | *4·2*(R) | *12*(L,R) | (CH) | N | Y | Edge HII (see text) | 3·3, 15·5 |
| 340·06 | −0·25 | 16 44 36·9 | −45 16 27 | 15 | −58, −48 | *12·0*(R) | 13·6(L) | — | RCG | N | Y | HII | 4·6, 14·2 |

[A] Range of radial velocity over which emission is detectable.
[B] Epoch 1978 August; transition(s) used for position determination given in italics.
[C] In parentheses if no profile is shown: RCG, Robinson *et al.* (1974); CH, Caswell and Haynes (1975); GMR, Goss *et al.* (1970); CHG, Caswell *et al.* (1977).
[D] Near and far distances are given; where there is evidence favouring one of these, it is given in italics.

*OH326·77−0·26*. The single feature (100% LH at 1665 MHz) seen in August 1978 was three times stronger than in July 1976. The position is poor, since it was measured when the source was weak; non-detection of $H_2O$ (our unpublished data) may thus be due to searching at an incorrect position. Weak 1667 MHz emission is probably present near our detection limit (0·4 Jy).

*OH327·29−0·58*. Strongly variable. At $V = -60\ \mathrm{km\,s^{-1}}$ no feature was detected in 1972 (RCG), then an RH feature with peak intensity of 4 Jy was discovered in July 1976, and by August 1978 it had flared to 22 Jy. The feature at $-54\ \mathrm{km\,s^{-1}}$ increased by a factor of 2 between July 1976 and August 1978. Features at −68·5 and $-71{\cdot}0\ \mathrm{km\,s^{-1}}$ detected in July 1976 resemble a 'Zeeman pair' and were not detected in August 1978 (see Fig. 2). A spectrum in March 1976 closely resembled that in July 1976. The HII region G 327·3−0·6 has a mean radial velocity which coincides with the prominent OH absorption at $V = -49\ \mathrm{km\,s^{-1}}$; weak 1612 MHz emission (probably spatially extended) also occurs at this velocity (CH).

*OH327·40+0·45*. This OH maser is in the same direction as the SNR G 327·4+0·4, whose distance (Clark and Caswell 1976; revised by Caswell and Lerche 1979) is estimated as 6 kpc. The distance of the maser is probably ~5·8 kpc (the near kinematic distance) so that the objects might be related, although the coincidence could be due to chance alone. No previous instance of main-line emission associated with SNRs has been proposed (see also the notes to OH 337·00−0·02), but in the case of two other SNRs, OH maser emission on the 1720 MHz transition is found nearby and is believed to be related to the SNRs (HC).

*OH328·24−0·54*. The intensity of the narrow 1667 MHz feature at $V = -38\ \mathrm{km\,s^{-1}}$ increased by a factor of 2 between July 1976 and August 1978. The peak intensity of the major features showed little change between 1970 (RCG) and 1978.

*OH328·30+0·44*. Emission at 1612 MHz occurs at $V = -95\ \mathrm{km\,s^{-1}}$ but is unpolarized and weak (0·6 Jy total intensity); it is likely to be spatially extended—type IIc emission as designated by CH—and hence a check for the presence of 1720 MHz absorption would be of interest.

*OH328·81+0·64*. Emission at 1612 MHz shows an RH peak of 6·5 Jy at $-44{\cdot}8\ \mathrm{km\,s^{-1}}$ and an LH peak of 5·0 Jy at $-45{\cdot}5\ \mathrm{km\,s^{-1}}$. This seems a likely candidate for interpretation as a pair of features split by the Zeeman effect, the line-of-sight magnetic field being ~5 mG. No corresponding pairs are apparent on the main-line transitions. The continuum source G 328·81+0·64 has $S_{5\mathrm{GHz}} = 1{\cdot}0$ Jy, and is of small diameter, <2′ arc (Haynes *et al.* 1979*a*); recombination-line measurements are needed to ascertain whether it is a compact HII region, as seems likely in view of its coincidence with the OH maser.

*OH329·04−0·21*. Near the source there is a large OH cloud giving rise to weak extended 1612 MHz emission (type IIc of CH). Note the proximity of the following source, which is less than one beamwidth away—when pointing at one source, the other is weakly detectable.

---

**Figs 1–17.** Profiles of OH main-line masers (at 1665 and 1667 MHz) in the survey region. The continuous thick line denotes the right-hand (RH) sense of circular polarization and the thin (dashed) line denotes the left-hand (LH). In all figures the intensity scale refers to one sense of polarization so that the total intensity is the sum (not the mean) of the intensities in each polarization. The velocity resolution is $0{\cdot}14\ \mathrm{km\,s^{-1}}$ (≡ 0·8 kHz). The profiles were observed in August 1978 except where otherwise noted.

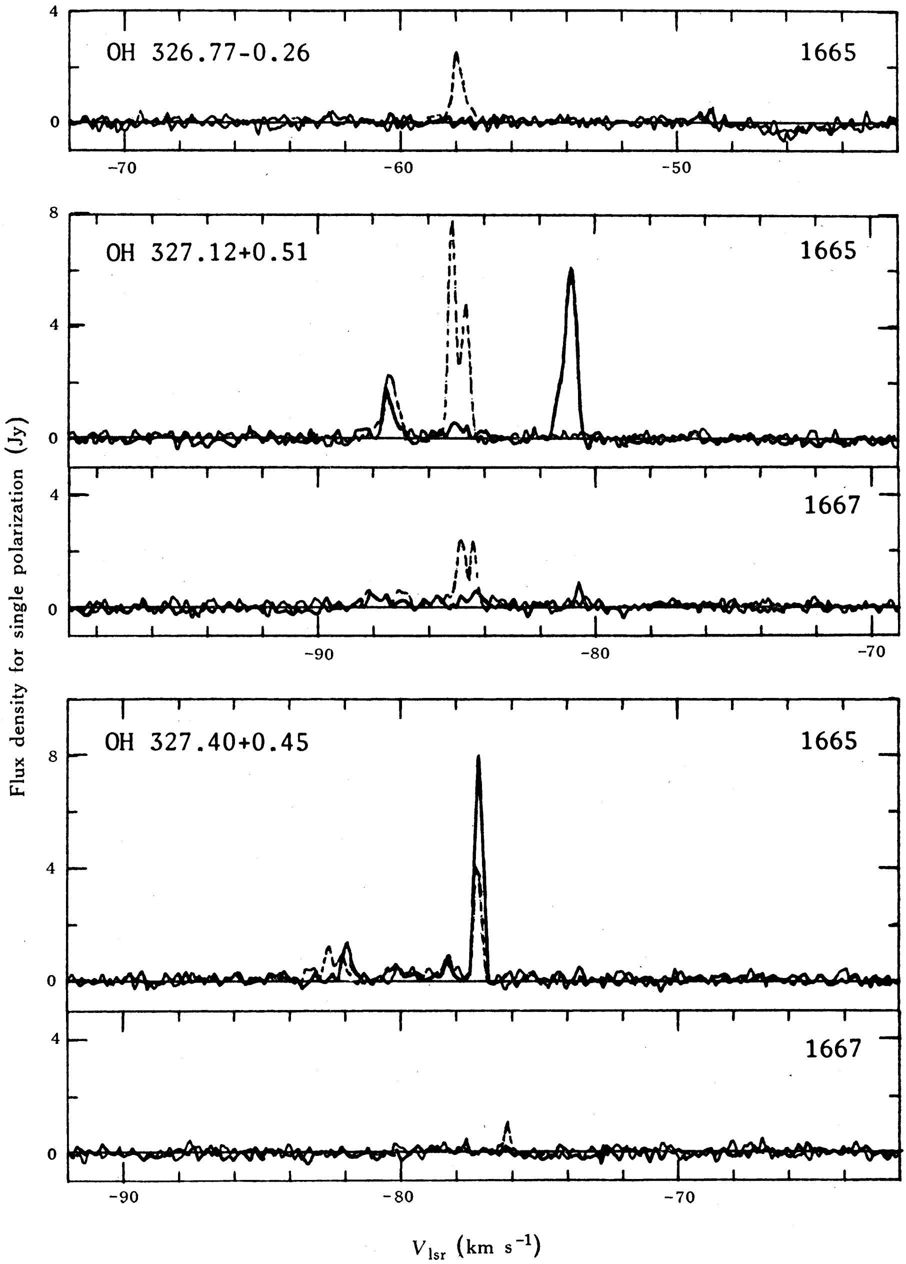

OH 326.77-0.26
1665
4
0
-70
-60
-50
OH 327.12+0.51
1665
1667
8
4
0
4
0
-90
-80
-70
OH 327.40+0.45
1665
1667
8
4
0
4
0
-90
-80
-70
Flux density for single polarization (Jy)
$V_{lsr}$ (km s$^{-1}$)


**Fig. 1**

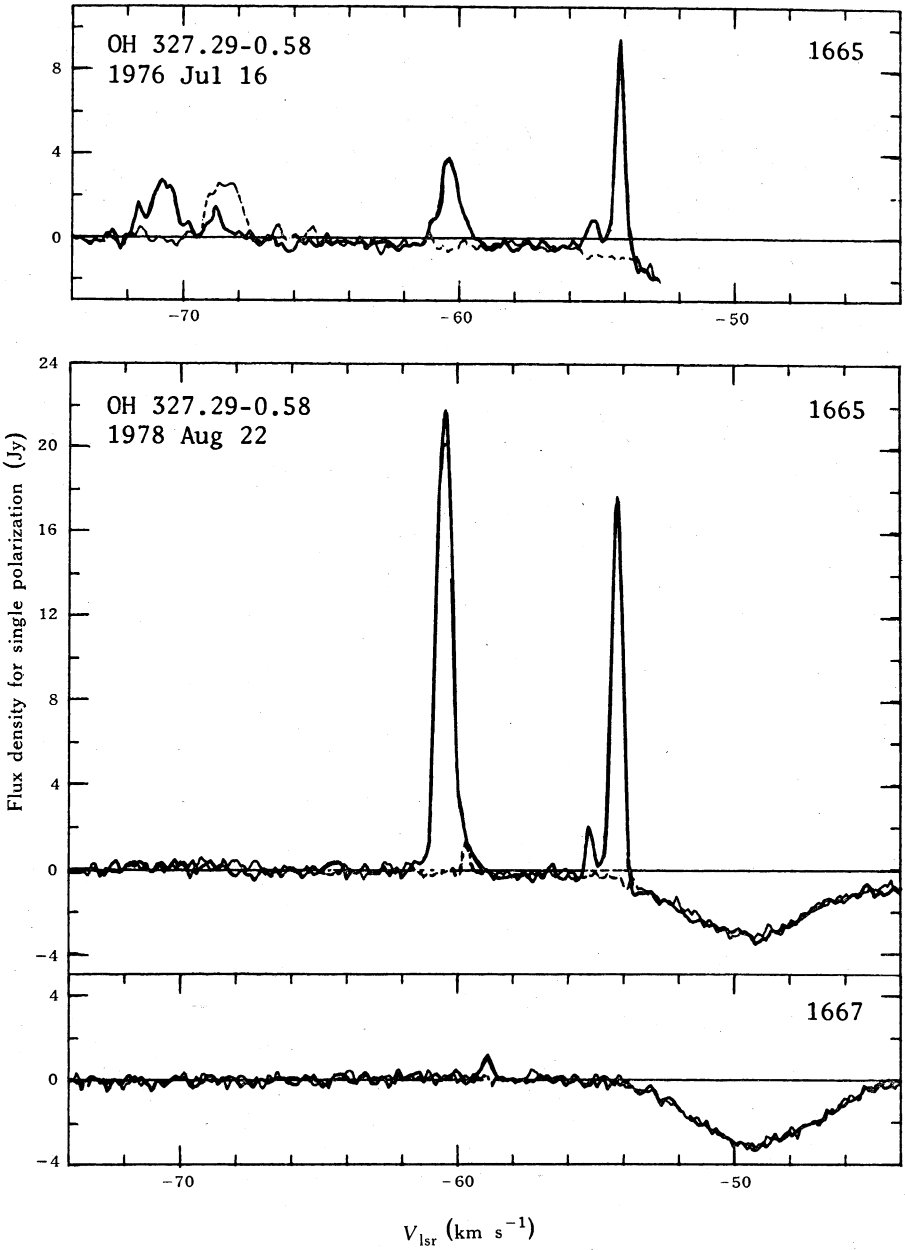
OH 327.29-0.58
1976 Jul 16
1665
8
4
0
-70
-60
-50
24
OH 327.29-0.58
1978 Aug 22
1665
20
16
12
8
4
0
-4
Flux density for single polarization (Jy)
4
1667
0
-4
-70
-60
-50
$V_{lsr}$ (km s$^{-1}$)

**Fig. 2**

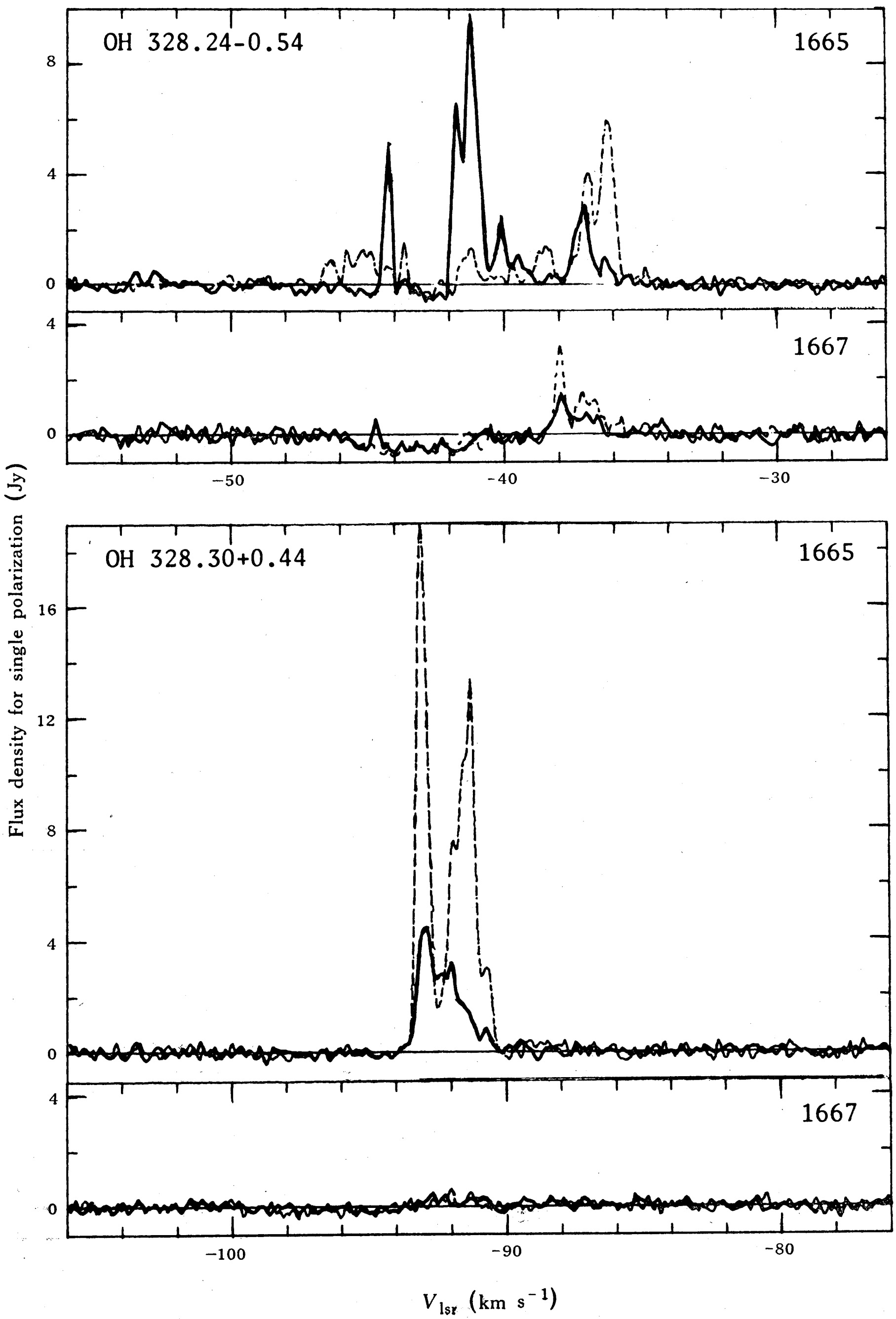
OH 328.24-0.54
1665
8
4
0
4
1667
0
-50
-40
-30
OH 328.30+0.44
1665
16
12
8
4
0
4
1667
0
-100
-90
-80
Flux density for single polarization (Jy)
$V_{lsr}$ (km s$^{-1}$)

**Fig. 3**

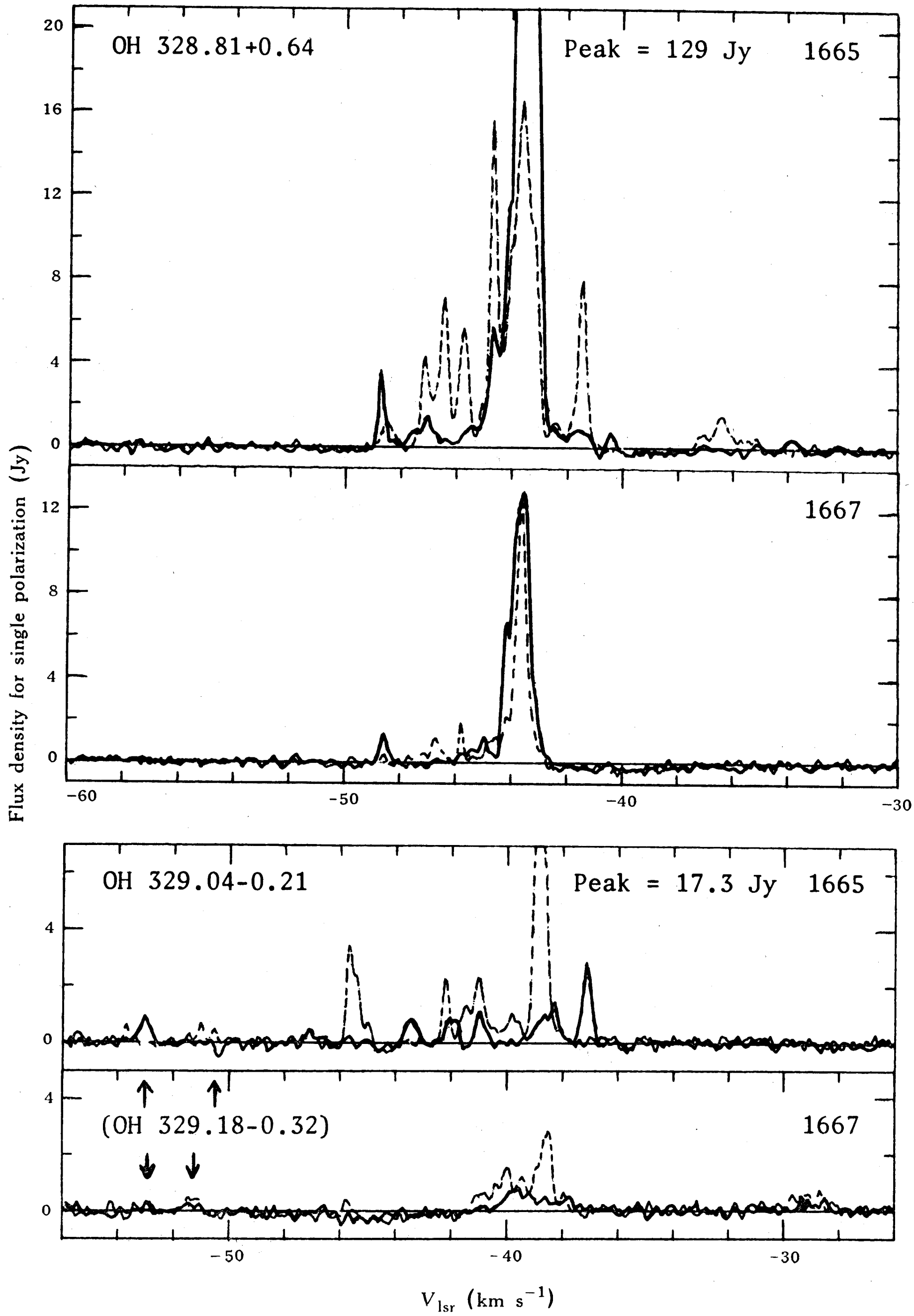

OH 328.81+0.64
Peak = 129 Jy
1665
1667
Flux density for single polarization (Jy)
OH 329.04-0.21
Peak = 17.3 Jy
(OH 329.18-0.32)
$V_{\rm lsr}$ (km $s^{-1}$)


**Fig. 4**

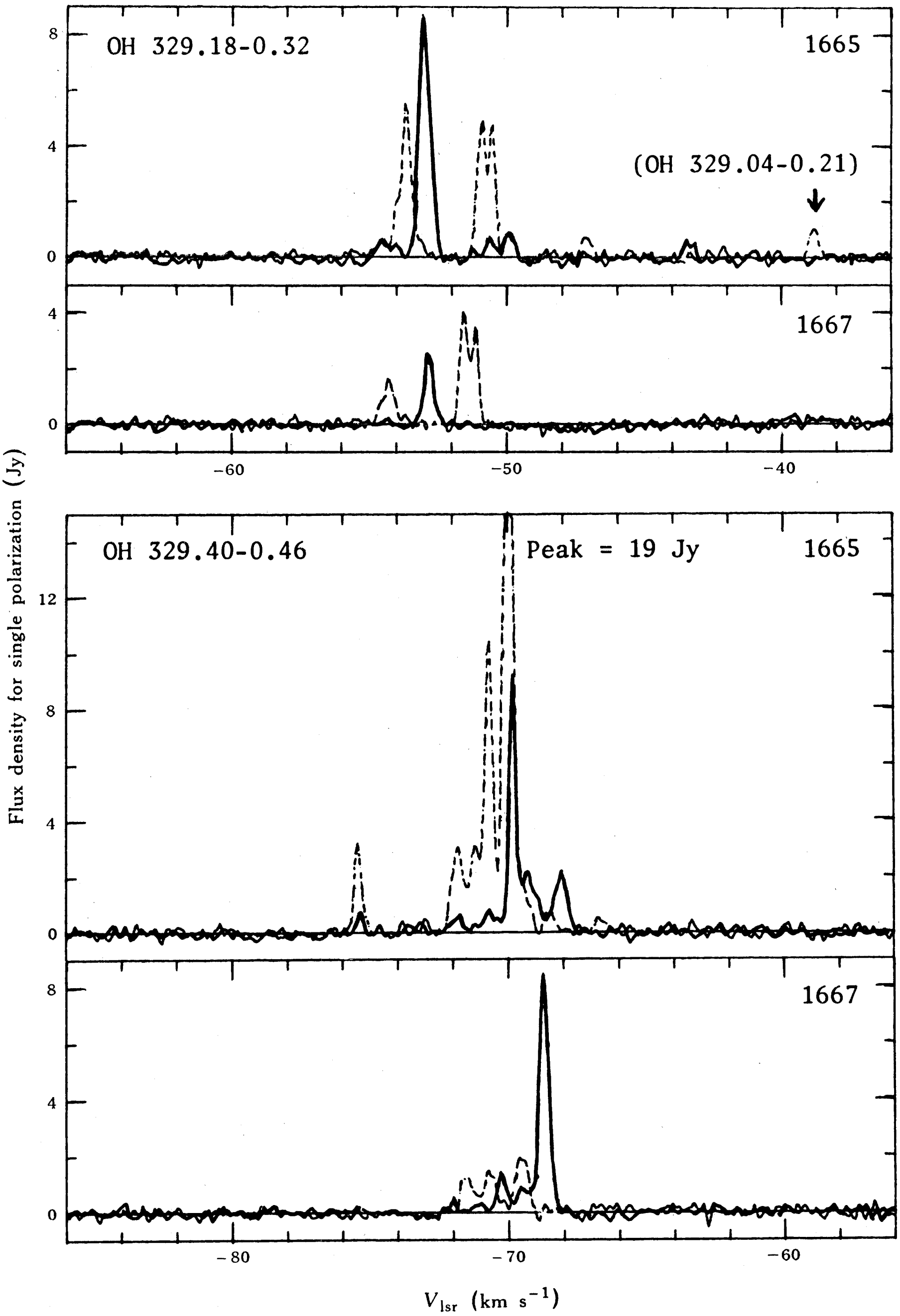
OH 329.18-0.32
1665
(OH 329.04-0.21)
1667
OH 329.40-0.46
Peak = 19 Jy
1665
1667
Flux density for single polarization (Jy)
8
4
0
4
0
-60
-50
-40
12
8
4
0
8
4
0
-80
-70
-60
$V_{lsr}$ (km $s^{-1}$)

**Fig. 5**

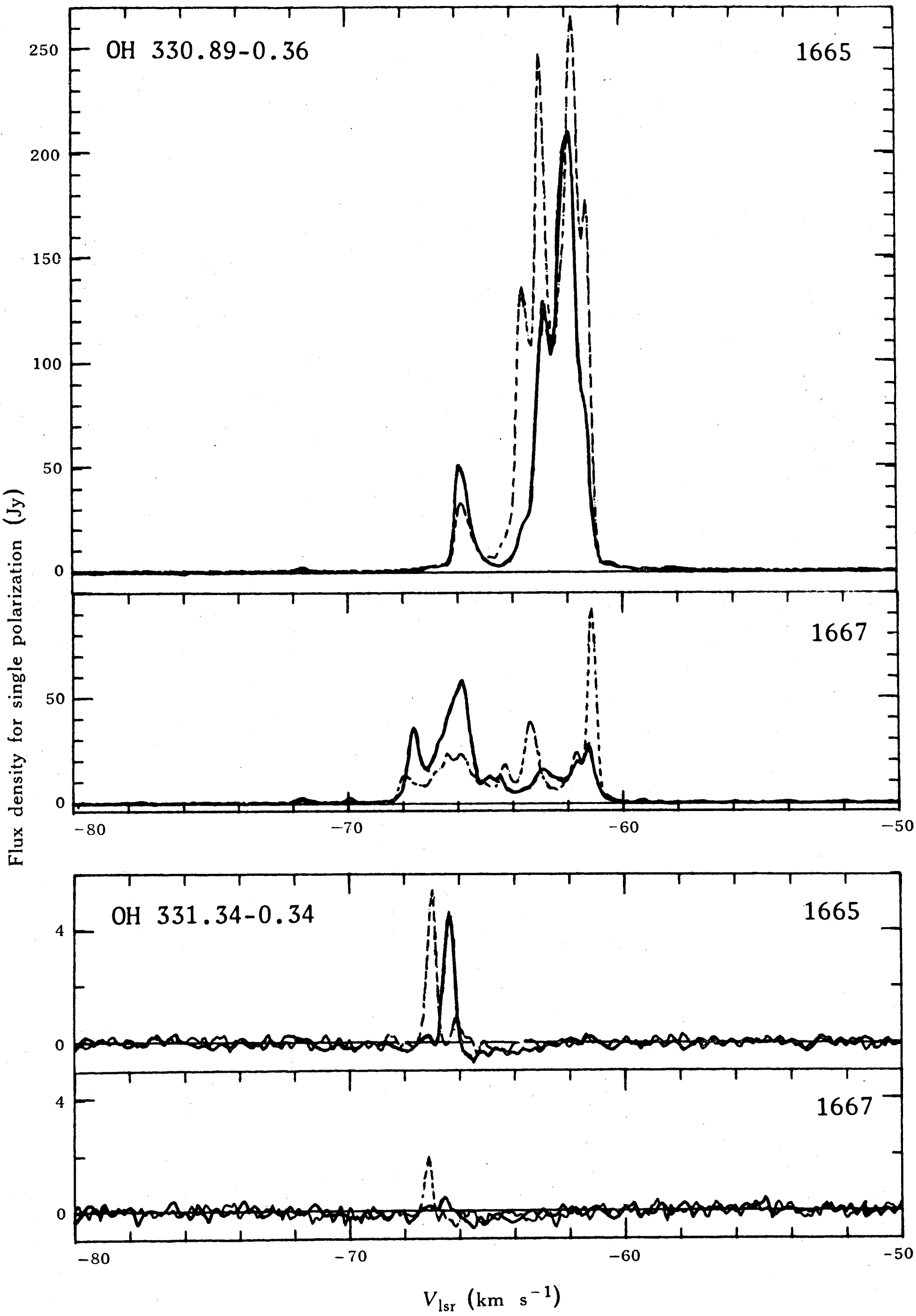

OH 330.89-0.36
1665
1667
OH 331.34-0.34
1665
1667
250
200
150
100
50
0
4
-80
-70
-60
-50
Flux density for single polarization (Jy)
$V_{lsr}$ (km s$^{-1}$)


**Fig. 6**

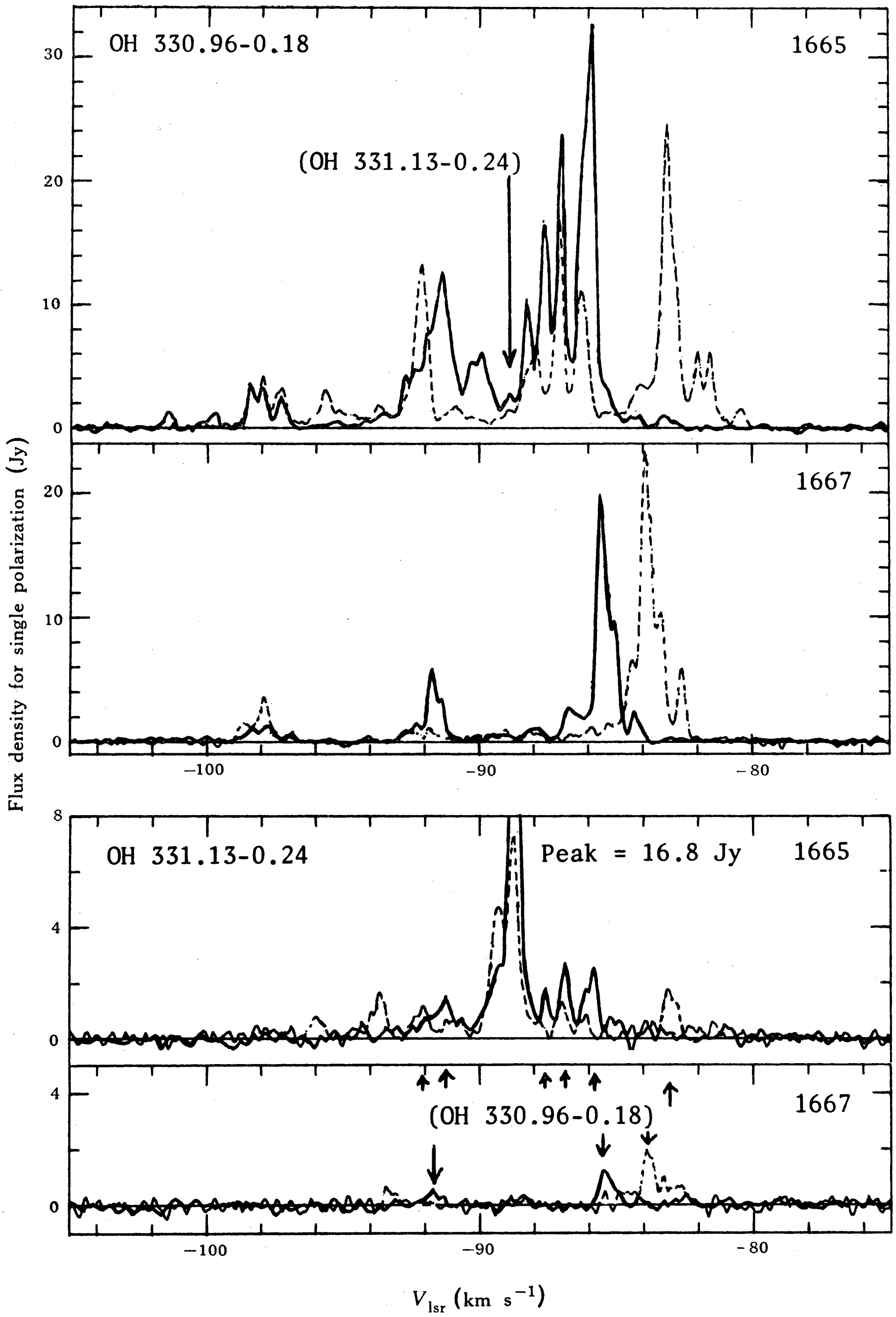
OH 330.96-0.18
1665
(OH 331.13-0.24)
1667
Flux density for single polarization (Jy)
OH 331.13-0.24
Peak = 16.8 Jy
1665
(OH 330.96-0.18)
1667
−100
−90
−80
$V_{lsr}$ (km s$^{-1}$)

**Fig. 7**

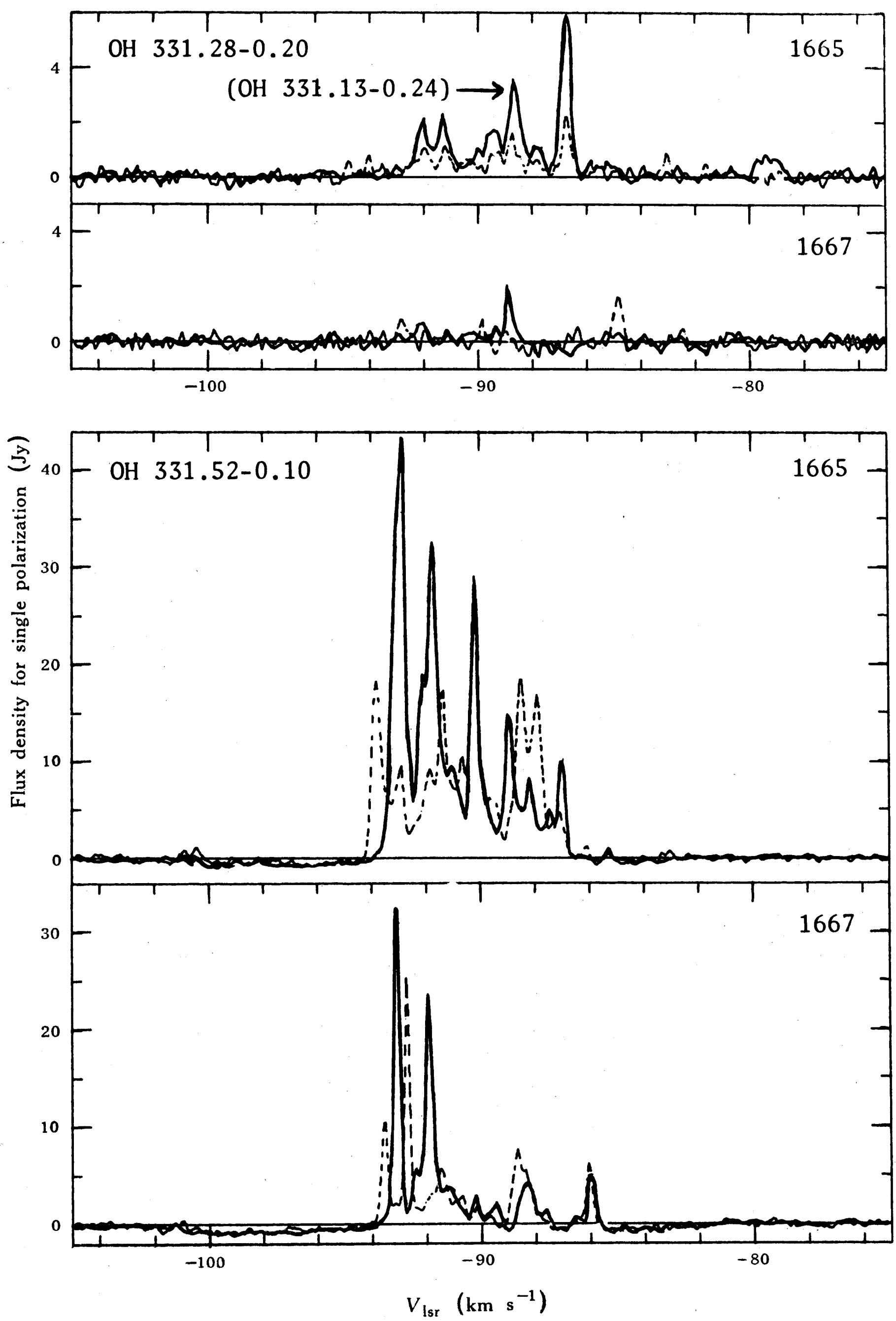
OH 331.28-0.20
1665
(OH 331.13-0.24)
1667
OH 331.52-0.10
1665
1667
Flux density for single polarization (Jy)
-100
-90
-80
$V_{lsr}$ (km s$^{-1}$)

**Fig. 8**

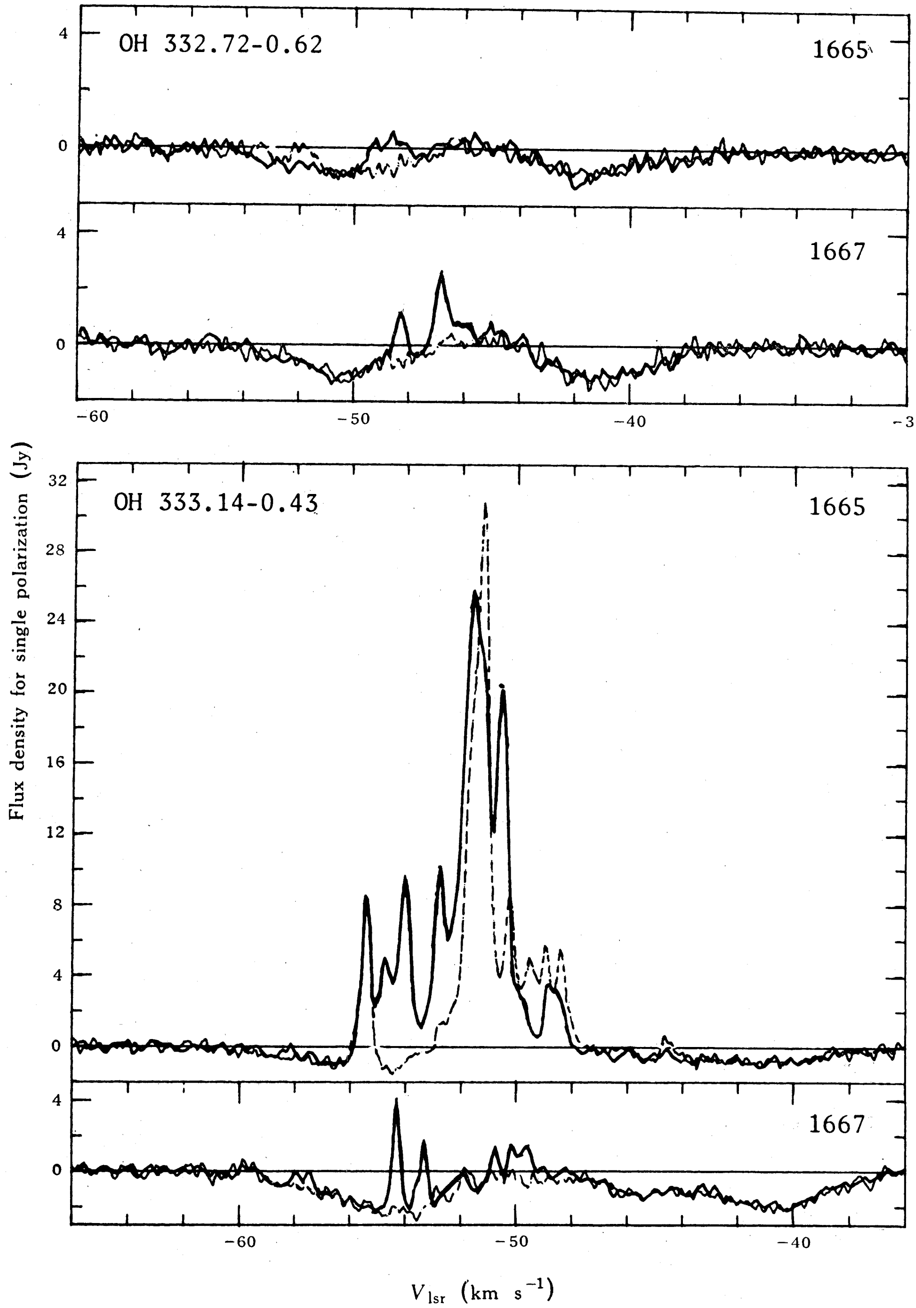
OH 332.72-0.62
1665
1667
OH 333.14-0.43
1665
1667
Flux density for single polarization (Jy)
$V_{lsr}$ (km s$^{-1}$)
4
0
4
0
-60
-50
-40
-30
32
28
24
20
16
12
8
4
0
4
0
-60
-50
-40

**Fig. 9**

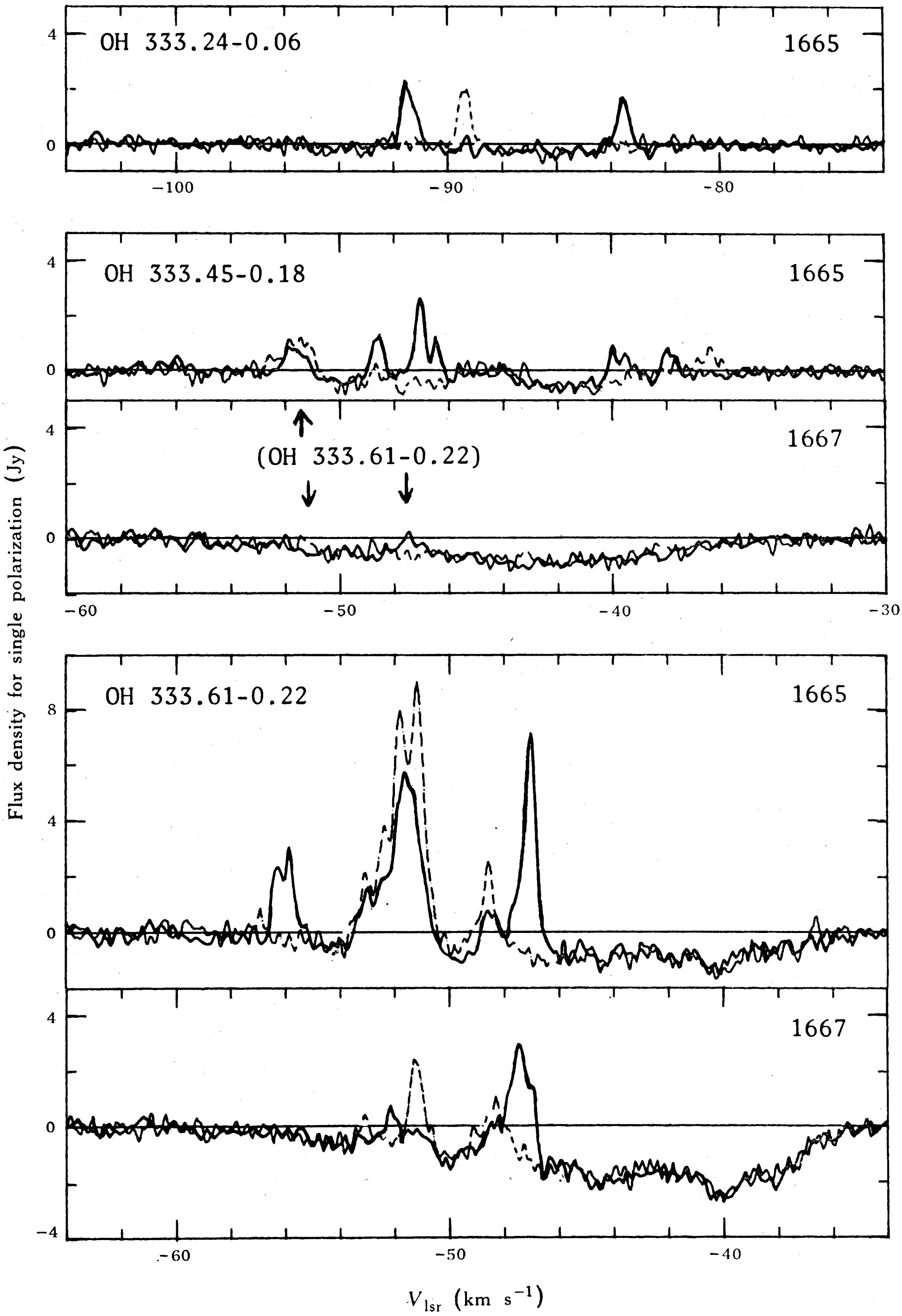
OH 333.24-0.06
1665
OH 333.45-0.18
1665
1667
(OH 333.61-0.22)
OH 333.61-0.22
1665
1667
Flux density for single polarization (Jy)
$V_{lsr}$ (km $s^{-1}$)

**Fig. 10**

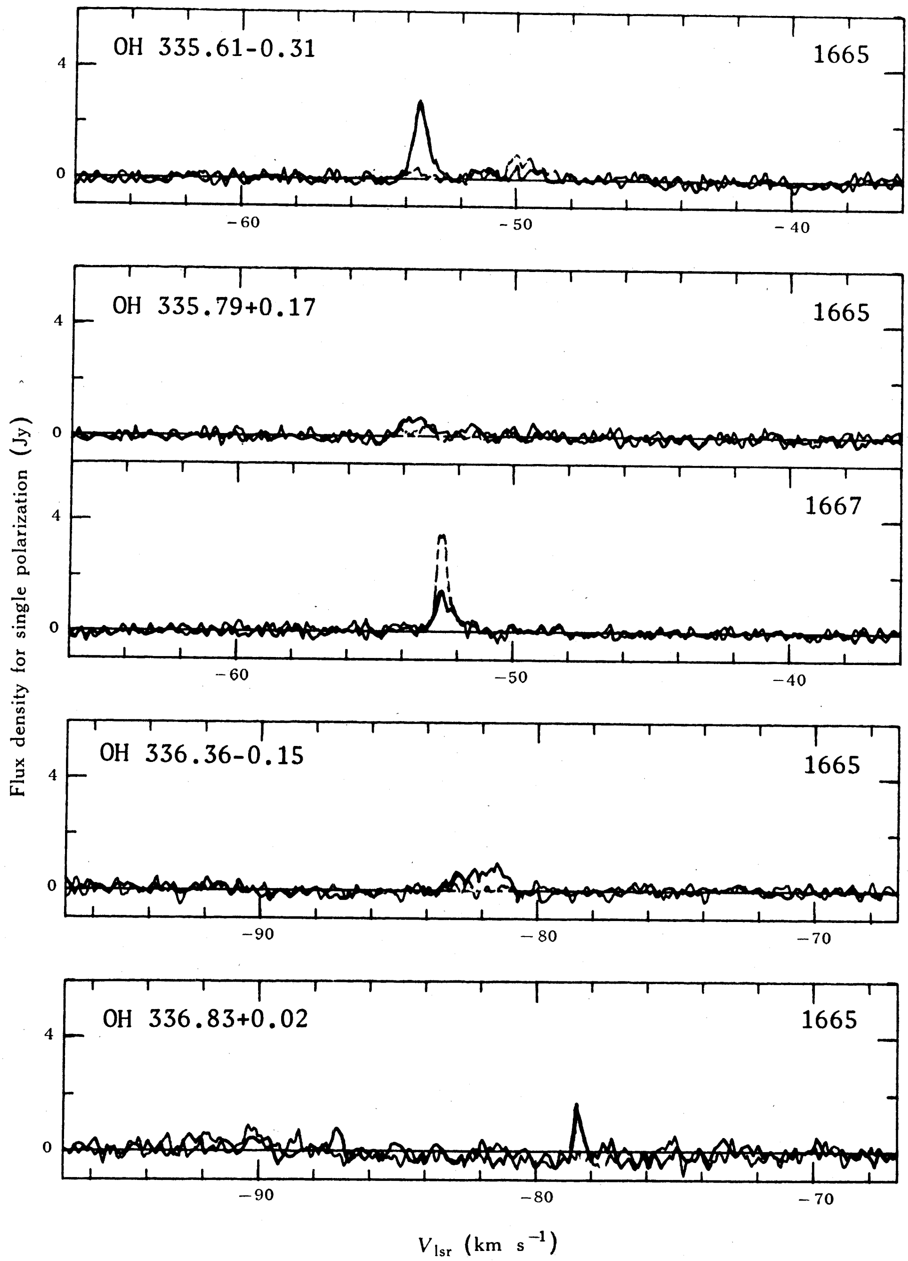
OH 335.61-0.31
1665
OH 335.79+0.17
1665
1667
OH 336.36-0.15
1665
OH 336.83+0.02
1665
Flux density for single polarization (Jy)
4
0
-60
-50
-40
-90
-80
-70
$V_{lsr}$ (km s$^{-1}$)

**Fig. 11**

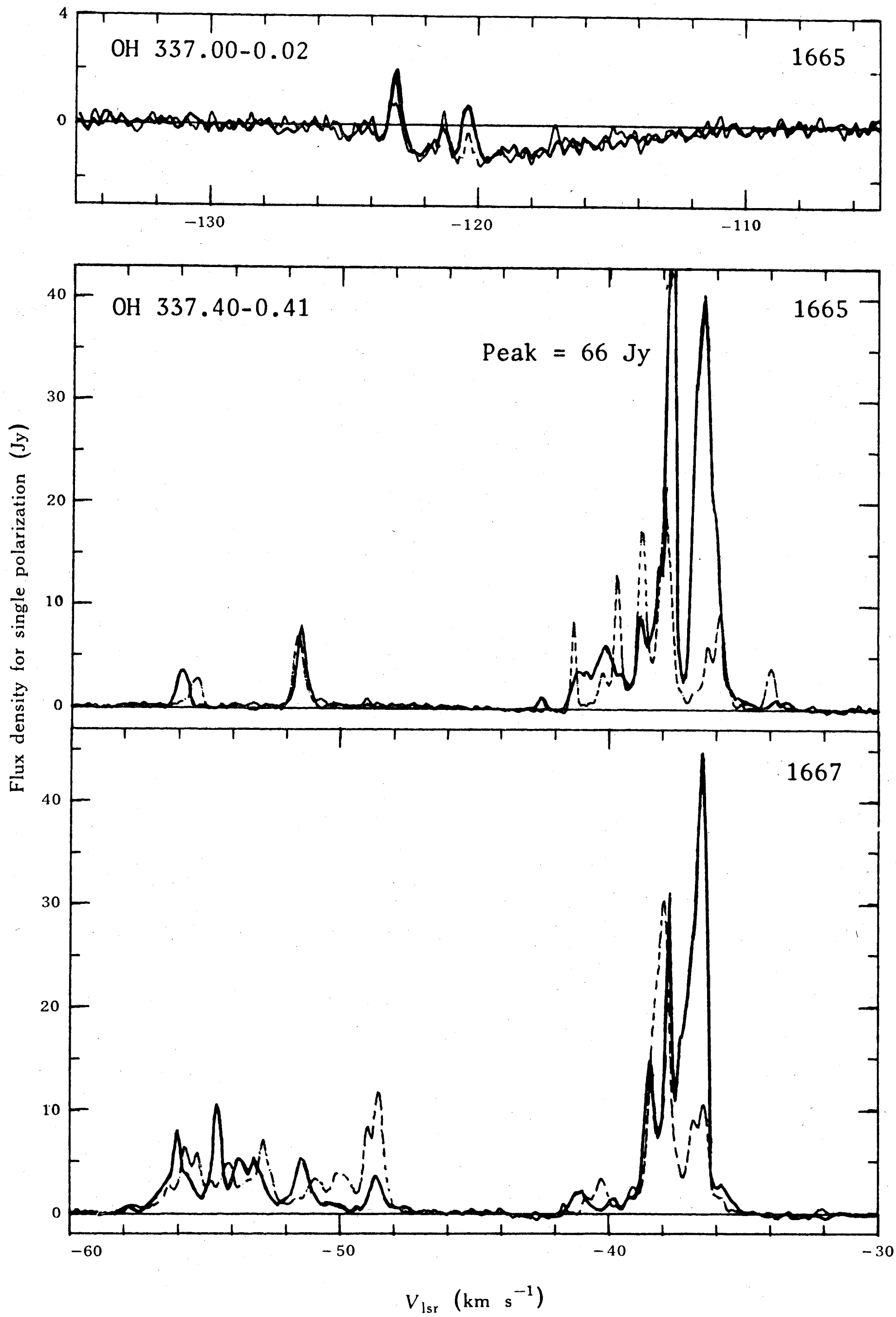
OH 337.00-0.02
1665
4
0
-130
-120
-110
OH 337.40-0.41
1665
Peak = 66 Jy
40
30
20
10
0
1667
Flux density for single polarization (Jy)
-60
-50
-40
-30
$V_{lsr}$ (km $s^{-1}$)

**Fig. 12**

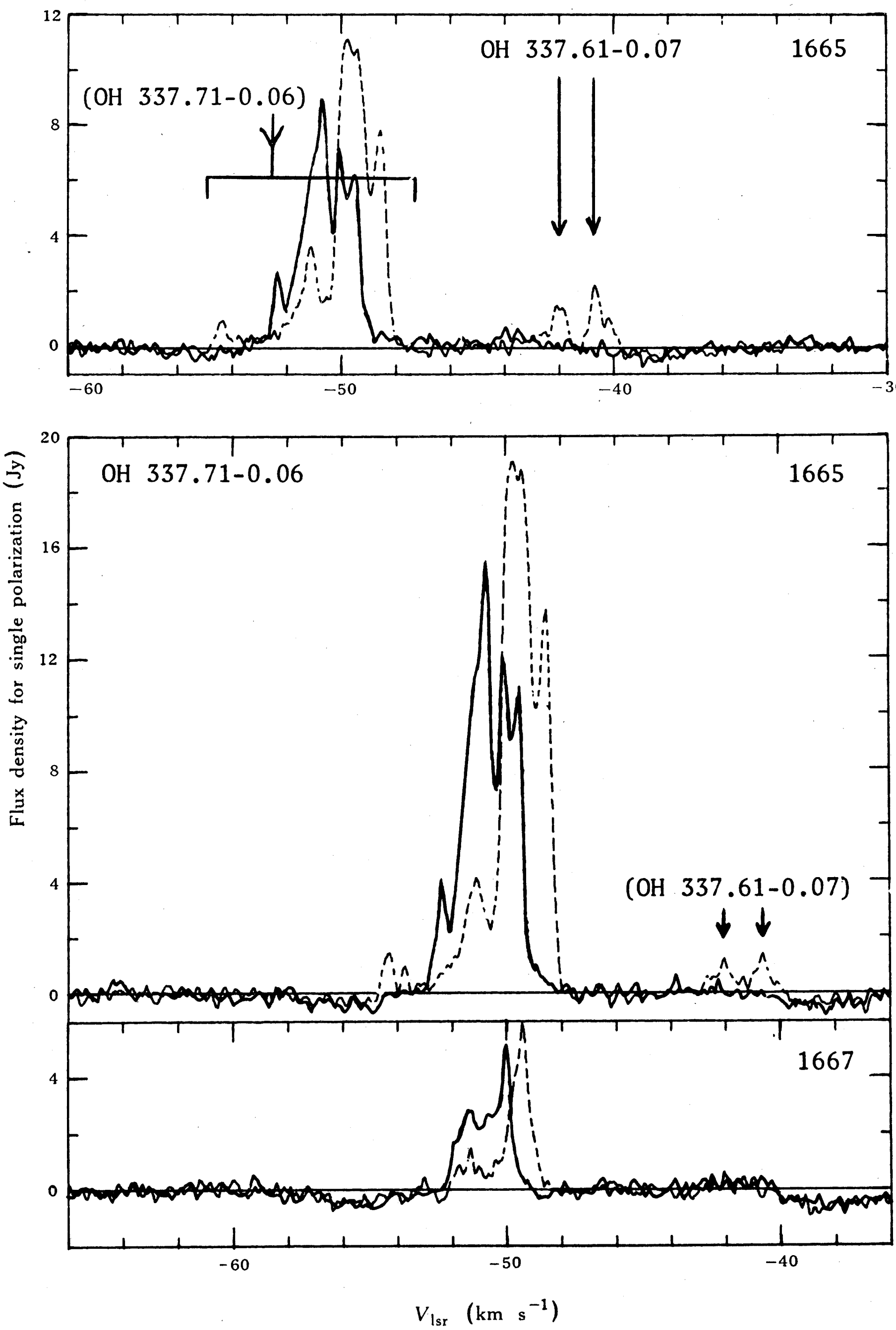
OH 337.61-0.07
1665
(OH 337.71-0.06)
OH 337.71-0.06
1665
(OH 337.61-0.07)
1667
Flux density for single polarization (Jy)
$V_{lsr}$ (km s$^{-1}$)

Fig. 13

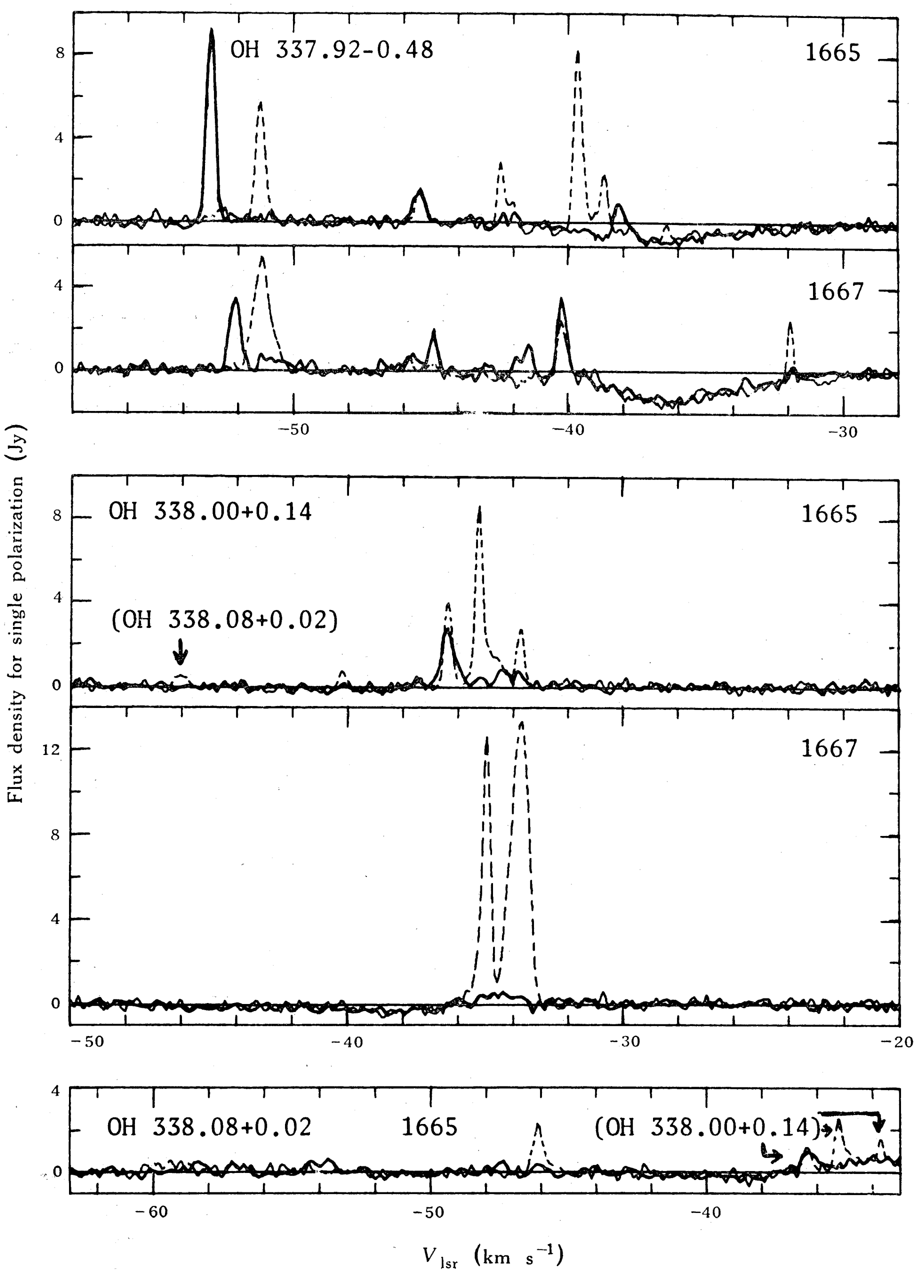
OH 337.92-0.48
1665
1667
OH 338.00+0.14
(OH 338.08+0.02)
1665
1667
OH 338.08+0.02
1665
(OH 338.00+0.14)
Flux density for single polarization (Jy)
V lsr (km s^-1)
8
4
0
4
0
−50
−40
−30
8
4
0
12
8
4
0
−50
−40
−30
−20
4
0
−60
−50
−40

**Fig. 14**

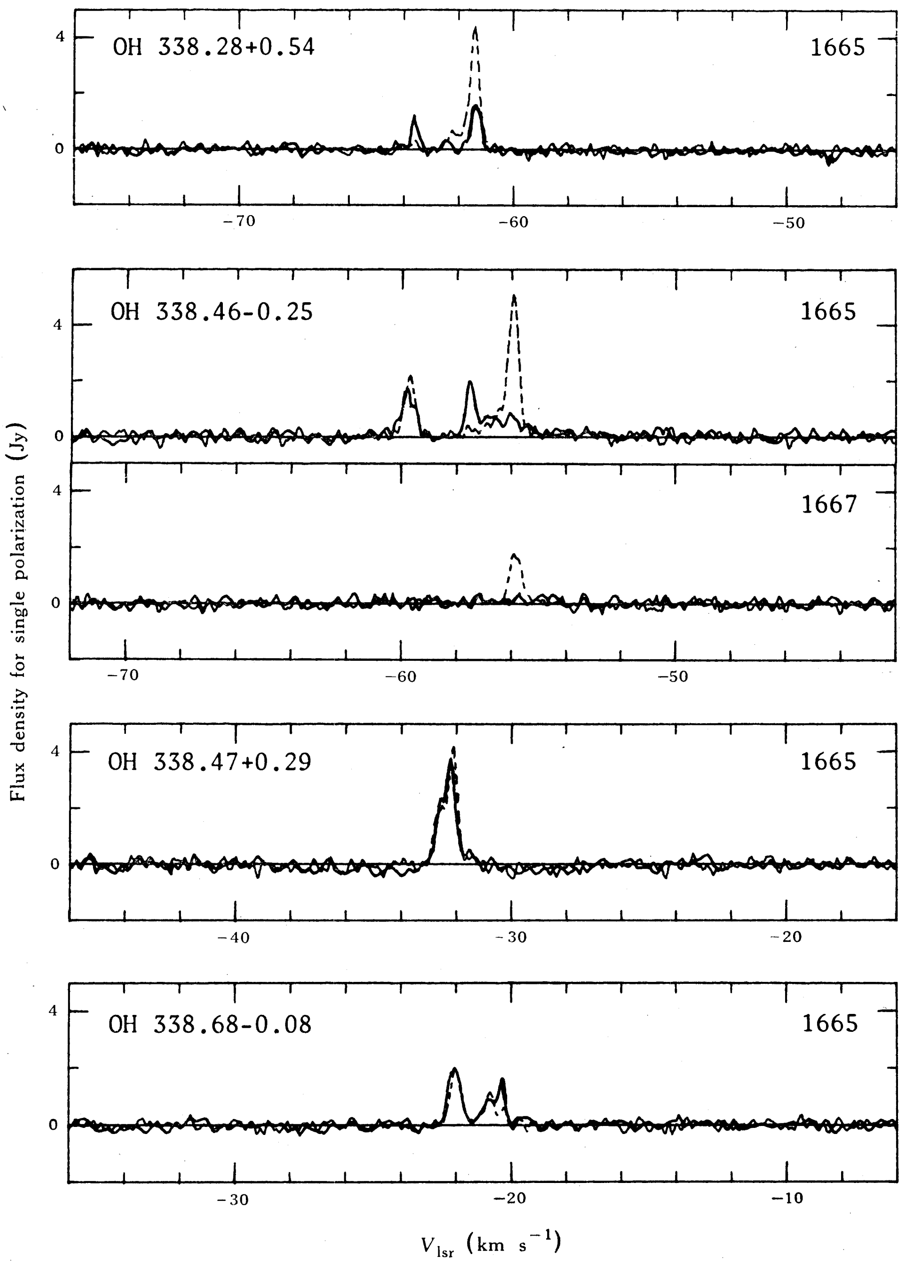
OH 338.28+0.54
1665
OH 338.46-0.25
1665
1667
OH 338.47+0.29
1665
OH 338.68-0.08
1665
Flux density for single polarization (Jy)
$V_{lsr}$ (km s$^{-1}$)

**Fig. 15**

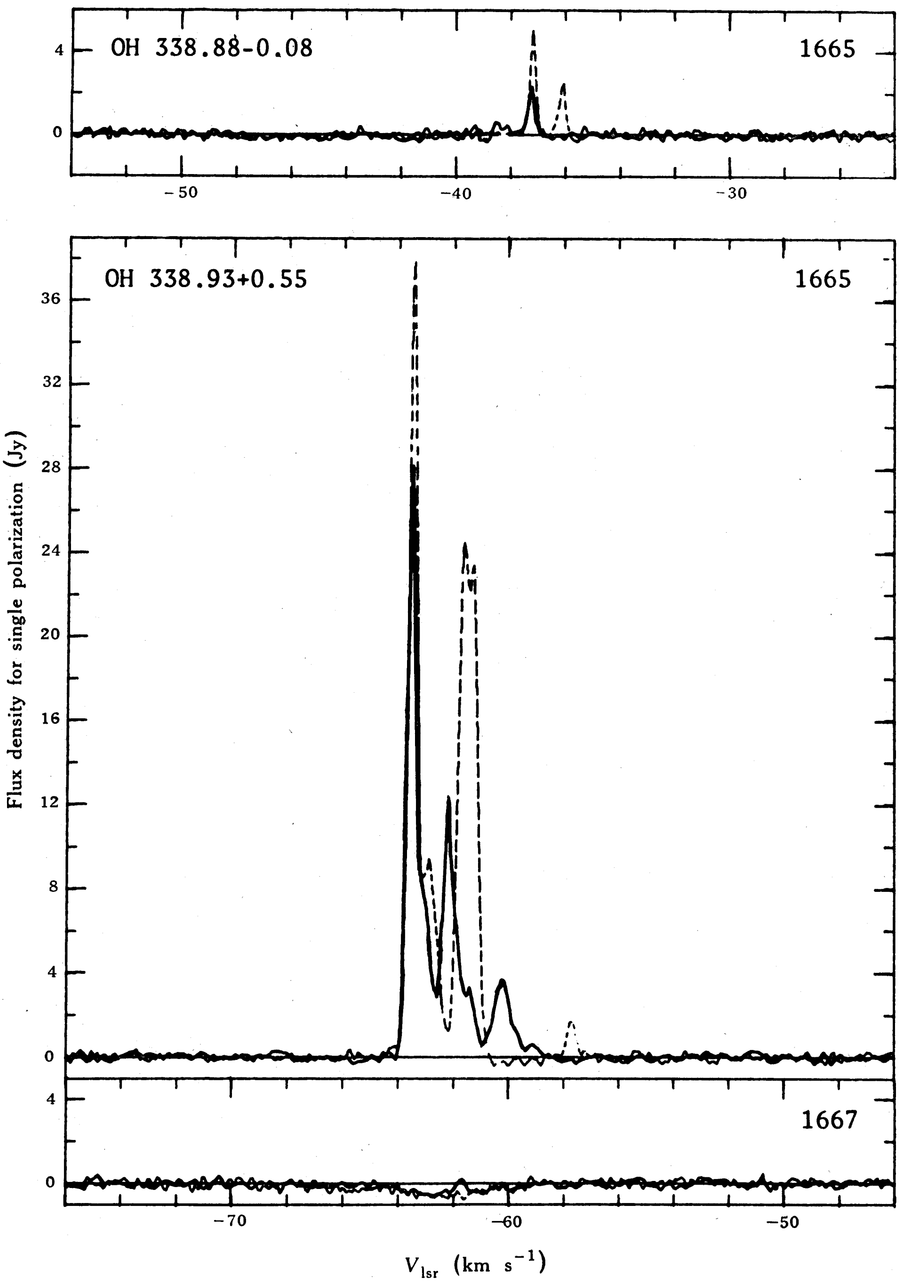
OH 338.88-0.08
1665
4
0
-50
-40
-30
OH 338.93+0.55
1665
36
32
28
24
20
16
12
8
4
0
Flux density for single polarization (Jy)
1667
4
0
-70
-60
-50
$V_{lsr}$ (km $s^{-1}$)

**Fig. 16**

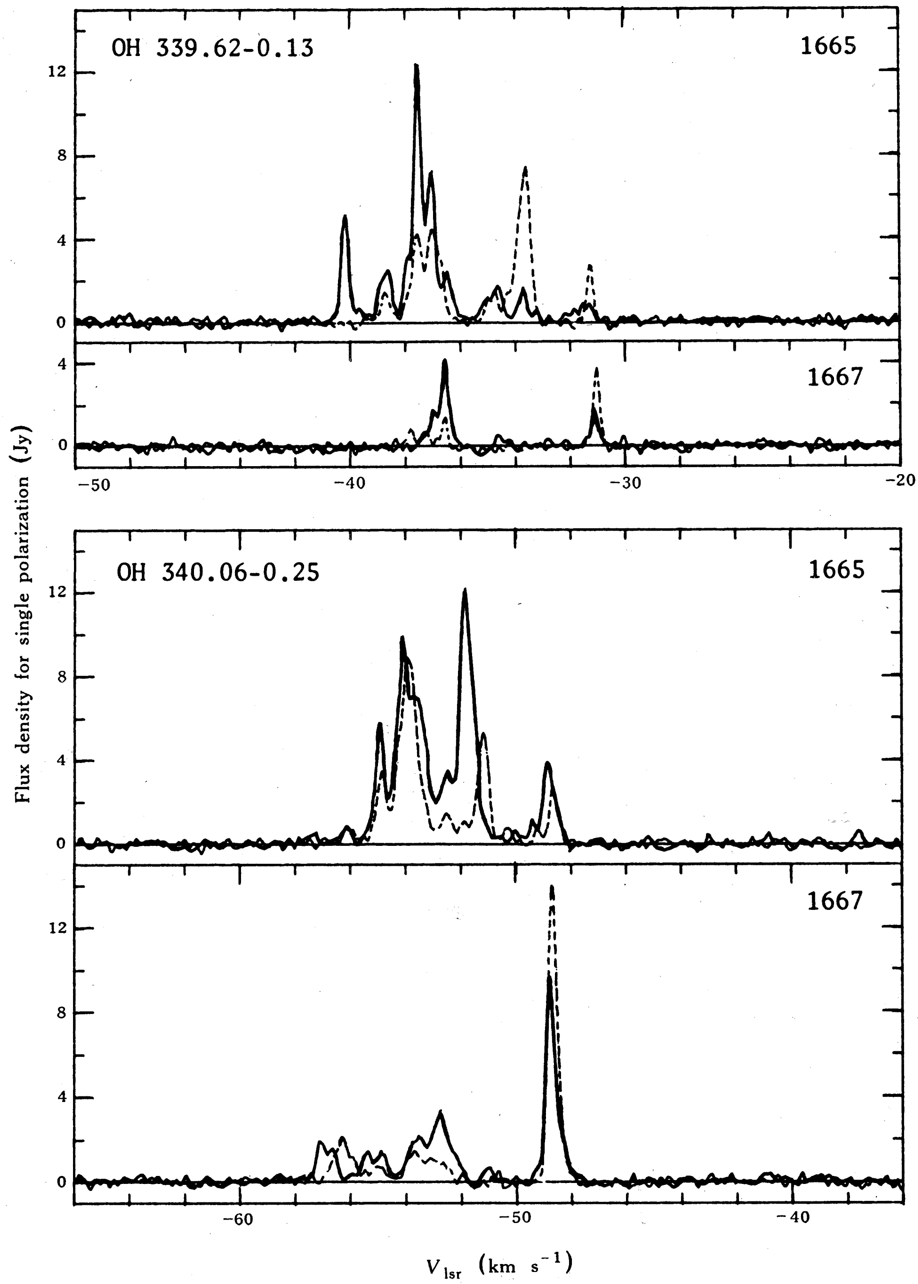
OH 339.62-0.13
1665
1667
OH 340.06-0.25
1665
1667
Flux density for single polarization (Jy)
12
8
4
0
-50
-40
-30
-20
-60
-50
-40
$V_{lsr}$ (km $s^{-1}$)

Fig. 17

*OH329·18−0·32.* The similar velocity structure and polarization of 1665 and 1667 MHz emission suggest that the masers of each transition may correspond closely in position, with the slight displacements in velocity due to Zeeman splitting.

*OH330·89−0·36.* This very strong maser showed essentially no changes (<10%) between July 1976 and August 1978. Indeed the much earlier filter bank observations of 1970 (RCG) are also very similar (the slightly larger changes may merely reflect the different uncertainties in calibrating strong signals in the filter bank and correlator). Note that there is weak extended 1612 MHz emission associated with this type I maser (CH).

*OH330·96−0·18.* Associated emission at 1612 MHz is weak and extended (CH). Note that OH 331·13−0·24 is less than one beamwidth away. The major LH and RH features at 1667 MHz are separated by $\sim 1\cdot 6\ \mathrm{km\,s^{-1}}$ and may result from Zeeman splitting in a field of 4·5 mG (line-of-sight component); the 1665 MHz spectrum is more complex but the separation of the main peaks is compatible with this interpretation.

*OH331·13−0·24.* Note that both the previous source and the following source are less than one beamwidth away.

*OH331·28−0·20.* The 1665 MHz feature at $-87\ \mathrm{km\,s^{-1}}$ was stronger by a factor of 2 in August 1978 compared with July 1976.

*OH331·34−0·34.* The simple 1665 MHz structure is suggestive of a 'Zeeman pair'. The 1667 MHz feature is slightly weaker now than in 1970 but in July 1976 it reached a peak of 8 Jy.

*OH331·52−0·10.* Between July 1976 and August 1978 intensity changes of only ~10% occurred; over the longer period from 1968 to the present, changes exceed 100% in the case of some features (see GMR). The most striking property of the source is its remarkably strong and highly polarized 1612 MHz emission (GMR).

*OH333·24−0·06.* Two features were seen in March 1976 on the 1612 MHz transition at velocities of −87 and $-91\ \mathrm{km\,s^{-1}}$; both were 100% LH polarized. The 1665 MHz emission changed considerably between July 1976 and August 1978: the feature at $V = -83\cdot 5\ \mathrm{km\,s^{-1}}$ increased by a factor of 2 and the feature at $V = -89\cdot 4\ \mathrm{km\,s^{-1}}$ by a factor >5 (undetectable in July 1976).

*OH333·61−0·22.* Note the adjacent source OH 333·45−0·18, which is less than one beamwidth away. At 1665 and 1667 MHz, OH 333·61−0·22 has shown little change since 1968 (GMR). The accompanying 1612 MHz emission is 100% RH circularly polarized.

*OH335·79+0·17.* Note that this source is several times brighter at 1667 MHz than at 1665 MHz.

*OH336·36−0·15.* This source is currently (August 1978) the weakest in our list but it was 50% stronger in July 1976.

*OH336·83+0·02.* The feature at $V = -78\cdot 5\ \mathrm{km\,s^{-1}}$ was twice as strong in August 1978 as it was in July 1976.

*OH337·00−0·02.* This source lies in the direction of a probable SNR, whose distance is estimated by Clark and Caswell (1976) as ~11 kpc. The kinematic distance of the OH maser (9·2 kpc) is compatible with the maser being associated with the SNR (compare with the above notes on OH 327·40+0·45, which also lies in the direction of an SNR). The nearest discrete HII region has a velocity of $-78\ \mathrm{km\,s^{-1}}$

and thus seems unlikely to be associated with the OH maser whose velocity is $-122\ \mathrm{km\,s^{-1}}$.

*OH337·40−0·41.* The velocity structure, displaying two regions of emission most intense near the outer edges of the profile, is reminiscent of OH/IR stars, but no 1612 MHz emission is detectable. Most features remained at the same intensity between July 1976 and August 1978, but the 1667 MHz feature at $V = -42\ \mathrm{km\,s^{-1}}$ was eight times stronger in July 1976 than in August 1978; it was $\sim 100\%$ LH polarized. The maser position is 2′ arc from a 'point' source which is nonthermal, with $S_{0\cdot 4} = 2\cdot 29$ Jy and $S_5 = 0\cdot 53$ Jy.

*OH337·61−0·07.* Note the proximity to OH 337·71−0·06.

*OH337·71−0·06.* This source has changed only slightly between 1970 and 1978. At both 1665 and 1667 MHz the polarization–velocity structures resemble effects from Zeeman splitting with a line-of-sight field of $\sim 2$ mG (i.e. a splitting of $1\ \mathrm{km\,s^{-1}}$ at 1665 MHz and $\sim 0\cdot 6\ \mathrm{km\,s^{-1}}$ at 1667 MHz).

*OH337·92−0·48.* Although most features have persisted from 1970 through until 1978 there have been large intensity variations (an order of magnitude in some cases). Between 1976 and 1978 several features varied by more than 50%. The features near $V = -52\ \mathrm{km\,s^{-1}}$ are suggestive of Zeeman splitting (at both 1665 and 1667 MHz with velocity separations of $\sim 2$ and $\sim 1\ \mathrm{km\,s^{-1}}$ respectively) in a line-of-sight field of $\sim 3$ mG.

*OH338·00+0·14.* Emission at 1667 MHz is slightly stronger than at 1665 MHz. A very extended cloud of OH includes this position and shows weak 1612 MHz emission of type IIc (CH).

*OH338·08+0·02.* Note the proximity of OH 338·00+0·14.

*OH338·28+0·54.* The feature near $V = -64\ \mathrm{km\,s^{-1}}$ was not detectable (less than one-third of its current value) in July 1976; the other feature is unchanged.

*OH338·46−0·25.* The apparently nearby weak HII region G 338·4−0·2 has a radial velocity of $-4\cdot 3\ \mathrm{km\,s^{-1}}$ (according to Wilson *et al.* 1970) and is thus presumably not associated with the OH maser, whose velocity is $-58\ \mathrm{km\,s^{-1}}$.

*OH338·93+0·55.* Most features have remained with similar intensity since 1970; the exception is at $V = -63\cdot 5\ \mathrm{km\,s^{-1}}$, which increased from 14 Jy in 1970 to 18 Jy in 1976 and reached 38 Jy by August 1978. Note that 1612 MHz emission is strong and polarized whereas 1667 MHz emission is weak.

*OH339·62−0·13.* The accompanying 1612 MHz emission (CH) has quite narrow velocity structure ($\sim 0\cdot 3\ \mathrm{km\,s^{-1}}$ width for each of several features which blend together) and essentially no net circular polarization. An adjacent continuum source is probably an HII region, and the possible significance of a nearby X-ray source is discussed elsewhere (Haynes *et al.* 1979*b*).

### (*c*) *Absorption*

Absorption was evident in many directions but it will not be discussed in detail. Emission sources are often seen to arise from an extended absorbing cloud of OH. Although most of the main-line absorption clouds show no striking departures from local thermodynamic equilibrium (i.e. $1 < T_{1667}/T_{1665} \leqslant 9/5$), in many cases they display anomalies on the satellite lines (already discussed elsewhere by CH and HC).

We list in Table 2 the main features of absorption detected; the tabulation is given as a finding list for future investigations.

**Table 2. Absorption by OH at 1667 MHz in galactic longitude range 326° to 340°**

| Galactic coordinates l (°) | b (°) | Position (1950) R.A. (h m s) | Dec. (° ′) | Radial velocity centre (km s⁻¹) | width (km s⁻¹) | Absorption depth $\Delta T_a$ (K) | Notes[A] | Refs[B] |
|---|---|---|---|---|---|---|---|---|
| 326·4 | −0·4 | 15 43 39 | −54 53 | −45 | 6 | 0·5 | | |
| 327·0 | −0·2 | 15 46 03 | −54 21 | −46 | 3 | 0·8 | | CH; HC |
| 327·0 | +0·0 | 15 45 13 | −54 12 | −57 | 6 | 1·0 | | CR |
| 327·2 | −0·4 | 15 47 59 | −54 23 | −50 | 5 | 0·6 | | CR; HC |
| 328·0 | −0·0 | 15 50 31 | −53 34 | −43 | 3 | 0·8 | | CH; HC |
| 328·4 | +0·2 | 15 51 44 | −53 10 | −45 | 7 | 1·0 } | 1 | |
| 328·4 | +0·2 | 15 51 44 | −53 10 | −92 | 4 | 0·6 } | | |
| 328·4 | +0·4 | 15 50 53 | −53 01 | −52 | 3 | 1·0 | | |
| 331·0 | −0·2 | 16 06 22 | −51 46 | −43 | 6 | 1·4 } | 2 | CH; HC |
| 331·6 | −0·0 | 16 08 20 | −51 13 | −43 | 6 | 1·2 } | | |
| 331·6 | −0·0 | 16 08 20 | −51 13 | −56 | 6 | 0·8 | | |
| 331·6 | −0·0 | 16 08 20 | −51 13 | −98 | 4 | 0·8 | | |
| 332·4 | +0·2 | 16 11 11 | −50 31 | −90 | 8 | 1·0 | 2 | CH; HC |
| 332·4 | −0·4 | 16 13 47 | −50 57 | −42 | 4 | 0·7 | 1 | CR |
| 333·2 | +0·0 | 16 15 40 | −50 07 | −90 | 6 | 0·6 | | |
| 333·2 | −0·4 | 16 17 25 | −50 24 | −54 | 6 | 3·0 | 2 | CH; HC |
| 333·2 | −0·4 | 16 17 25 | −50 24 | −40 | 4 | 2·6 } | 2 | CH; HC |
| 333·6 | −0·2 | 16 18 19 | −49 59 | −40 | 4 | 3·0 } | | |
| 333·2 | +0·0 | 16 15 40 | −50 07 | −48 | 6 | 0·6 | | |
| 335·8 | −0·2 | 16 27 45 | −48 24 | −118 | 5 | 1·2 | | HC |
| 336·6 | +0·4 | 16 28 26 | −47 25 | −35 | 3 | 0·7 | | |
| 336·8 | +0·2 | 16 30 07 | −47 24 | −74 | 5 | 1·2 | 2 | CH; HC |
| 336·8 | +0·0 | 16 30 58 | −47 32 | −122 | 5 | 4·6 | 3 | CH; HC |
| 336·8 | +0·0 | 16 30 58 | −47 32 | −38 | 5 | 3·4 | 4 | CH; HC |
| 336·8 | +0·0 | 16 30 58 | −47 32 | −4 | 1 | 2·1 | | CR |
| 336·8 | +0·0 | 16 30 58 | −47 32 | −51 | 2 | 1·4 | | |
| 337·0 | +0·0 | 16 31 47 | −47 24 | −20 | 3 | 0·8 | | CR |
| 337·2 | +0·0 | 16 32 35 | −47 15 | −66 | 6 | 0·6 | | CH |
| 338·0 | +0·0 | 16 35 44 | −46 39 | −90 | 6 | 0·8 | | |
| 338·4 | +0·2 | 16 36 26 | −46 14 | −4 | 1 | 1·3 | | |
| 338·4 | +0·2 | 16 36 26 | −46 14 | −36 | 8 | 1·6 | | |
| 338·6 | +0·0 | 16 38 04 | −46 13 | −78 | 6 | −1·2 | | CH; HC |

[A] Notes: 1, supernova remnant; 2, extended absorption; 3, at velocities between −118 and −128 km s⁻¹, absorption very extended from 336°·4 to 338°·4 longitude; 4, at velocities between −38 and −44 km s⁻¹, absorption very extended from 334°·2 to 338°·4 longitude.

[B] References: CH, Caswell and Haynes (1975); HC, Haynes and Caswell (1977); CR, Caswell and Robinson (1974).

## 4. Discussion

### (*a*) *Luminosity Function for 1665 MHz Masers and Number of OH Masers in Galaxy*

The feasibility of this investigation is suggested by the unbiased nature of our search. As will become clear, this first attempt also reveals the major uncertainty which needs to be resolved for future improvements—distance estimates for more of the sources rather than more sources (40 are now available). The procedures for such investigations have previously been applied to such varied objects as extragalactic radio sources, pulsars, supernova remnants and the 1612 MHz OH masers associated with late-type stars.

We first define a convenient measure of luminosity $L = Sd^2$, where $S$ is the peak flux density in Jy and $d$ is the distance in kps; $L$ is therefore the peak flux which would be received from the source if its distance were 1 kpc (this is as adopted for type II OH/IR stars by CH and subsequently used by Johannson *et al.* 1977 and Bowers 1978). Unfortunately, unique distances are available for only 5 masers in our sample, with an ambiguity between a 'near' and a 'far' kinematic distance present for the remaining 35. For these ambiguous distances we therefore explored two extreme alternatives: (i) all are at the near distances; (ii) all are at the far distances. We approximate our sensitivity limit by a limiting cutoff at 1 Jy (the limit is strictly a probability function with steadily decreasing chance of detecting sources with $S < 1$ Jy, depending on the source position relative to our search grid). For very luminous sources our sensitivity limit would permit detection as far as the edge of the Galaxy. For less luminous sources we are sensitive over a somewhat smaller distance range and the observed numbers can be 'corrected' to estimate a true mean space density. For this region of the Galaxy we assume, as a crude approximation, that sources are distributed uniformly in a thin disc out to a distance of 15 kpc (corresponding to approximately 8 kpc galactocentric radius). Thus the number of sources with observed flux density $S$ at a distance $d$ has to be increased by the factor $225/Sd^2$ if this factor exceeds unity.

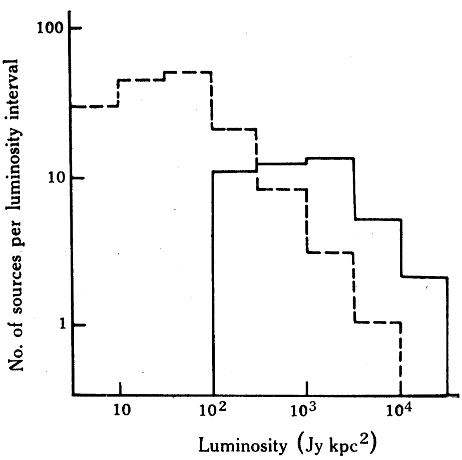


**Fig. 18.** Luminosity function for OH masers at 1665 MHz. The continuous and dashed lines are alternative histograms assuming sources are at far or near kinematic distances respectively. Number of sources relates to the survey region ($\sim 1/7 \cdot 2$ of whole Galaxy), with corrections for incompleteness at low luminosity (see Section 4*a* of the text).

Fig. 18 shows the luminosity function. For values of $L$ exceeding 100 Jy kpc$^2$ the function is quite well defined and the total number of sources estimated to be above this limit only differs by $\sim 30\%$ depending on whether 'near' or 'far' distances are adopted. Below $L = 100$ Jy kpc$^2$ the distance ambiguity is responsible for large uncertainties. There might either be no additional weak sources at all, or at the other extreme the number of sources with $L > 3$ Jy kpc$^2$ may be five times the number with $L > 100$ Jy kpc$^2$. The median value of luminosity is either approximately 30 or 1000 Jy kpc$^2$, depending on the distance ambiguity. If we allow for the limited fraction of the Galaxy searched ($\sim 1/7 \cdot 2$), then throughout the Galaxy there are probably $\sim 250$ sources with $L > 100$ Jy kpc$^2$ and in the range $3 < L < 100$ Jy kpc$^2$ there may either be very few masers or as many as 1000.

Another major class of main-line OH maser comprises the Mira variables. Their typical luminosity is low, $L \lesssim 1$ Jy kpc$^2$, and none appear in the present survey. It will be important to analyse their space density in a similar manner in order to assess whether they are separated from the masers investigated here by a distinct minimum in the luminosity function. A crude estimate, based on data tabulated by Bowers and Kerr (1977), suggests that throughout the Galaxy there may be well over 1000 Miras giving rise to type I OH emission with luminosity $\sim 1$ Jy kpc$^2$.

Both OH main-line masers and $H_2O$ masers are believed to be indicative of the sites of star formation; thus another comparison of interest is with the numbers of $H_2O$ masers in the Galaxy. Genzel and Downes (1979) suggest that there may be as many as 2000 $H_2O$ masers with $L > 10^{-8} L_{\odot}$, but there could be enormous uncertainties in this estimate in view of the very indirect manner in which it was derived. Nonetheless, with further refinements we may expect to learn whether a phase of both $H_2O$ and OH maser emission invariably accompanies star formation, and what the typical lifetimes of these phases are.

### (*b*) *Relative Intensities of the Four Ground-state Transitions*

The present results, in conjunction with our earlier satellite-line surveys, cover all four of the ground-state transitions in the survey region. For sources selected as emitters on the main lines (at either 1665 or 1667 MHz), we find that the intensity at 1665 MHz in 36 out of 40 cases exceeds that at 1667 MHz, the median intensity ratio being $\sim 3$. The largest ratio is $\sim 54$ (none of the lower limits imply ratios larger than this), the smallest ratio is 1/6, and thus the range is approximately a factor of 20 relative to the median ratio. Earlier surveys showed the same trends but with less confidence, since most of these surveys were biased towards the detection of 1665 rather than 1667 MHz emission.

Of the 40 sources, 6 show prominent 1612 MHz maser emission; some of these are associated with a high ratio of 1665 to 1667 MHz emission and some the reverse. At the approximate position (both in space and in velocity) of a further 5 main-line masers, there is weak 1612 MHz emission, which is probably spatially extended (type IIc of CH); the main-line maser probably arises from a small region embedded within the extended cloud.

### (*c*) *Polarization Characteristics*

Features showing a large percentage (up to 100%) of circular polarization commonly occur and this striking property of main-line OH masers apparently results from the presence of a magnetic field which causes Zeeman splitting. In a number of individual instances (see notes to sources in Section 2*b*) we have drawn attention to pairs of features, sometimes occurring on both transitions, which are compatible with the Zeeman interpretation and which can be used to estimate the line-of-sight magnetic field in the emitting region. The tendency for the two polarization components to be grossly unequal in intensity (such that one feature is commonly 'lost') must be accounted for in any adequate interpretation. The means of suppressing one sense of polarization at the expense of the other is not wholly clear. However, Cook's (1975) 'filter' mechanism—whereby line-of-sight gradients in velocity and magnetic field combine in such a way as to compensate, yielding a long path for coherence, at one polarization (frequency) but rapidly destroying coherence on the other polarization (slightly displaced frequency)—clearly operates in principle and seems to adequately account for the observations.

We also note the following new facts which could be regarded as evidence supporting Cook's (1975) model: in a number of sources one sense of polarization dominates on one of the main-line transitions; in most of these the same sense of polarization tends to dominate the other main-line transition. This could be accounted for in Cook's model if gradients of magnetic field and velocity do not change sign over most of the emitting region. In the extreme example of OH 205·12−14·11 (outside the present survey) we found that the emission at both 1665 and 1667 MHz was wholly left circular and the time variability (leading to eventual disappearance by April 1977) was similar on both transitions.

### (*d*) *Variability*

Studies by Sullivan and Kerstholt (1976) and Davies *et al.* (1977) have traced the history of several strong OH masers over a number of years. Our data are complementary to theirs in that our observation epochs are few (in many cases, only two, spaced two years apart), but these sources are a complete representative sample over a wide range of luminosity. Furthermore, during our observations the equipment remained essentially unchanged, which obviates many of the uncertainties encountered by Sullivan and Kerstholt in their attempts to abstract data from the literature. We searched 180 features for variability and 37% showed intensity variations exceeding 20% in the two year interval. For individual sources showing a large number of features it is possible to assess whether an above-average number of the features are variable: the only sources with strong indications of above-average variability were OH 327·29−0·58 and OH 337·92−0·48. To a good approximation, variability is equally common on the 1667 and 1665 MHz transitions. The number of intensity increases was roughly equal to the number of decreases and the slight asymmetry could readily be accounted for by an uncertainty in relative gain calibration of a few per cent. In the same period, different features within a single source are often found to vary markedly in opposite senses. This might be thought to imply a pumping mechanism local to each feature rather than a 'global' pump; but this is not necessarily so since, if Cook's (1975) filter mechanism favouring one sense of circular polarization operates, changes in velocity gradients and magnetic field gradients could be responsible for the intensity changes. With this latter interpretation, intensity changes in one polarized feature of a Zeeman pair are likely to be correlated inversely with the changes in the other component. Such 'anticorrelated' changes are observed in several sources where we have remarked on the apparent Zeeman pattern; it will be important to reassess this result when more statistics become available.

### (*e*) *Classification of OH Masers and their Association with Other Celestial Objects*

Subsequent to Turner's (1969) preliminary classification scheme of type I (main-line predominant) and type II (satellite-line predominant) sources, several *ad hoc* additions have been made. While the classification scheme clearly needs to be overhauled, it seems premature to do this at this time; an understanding of the origin of the pumping mechanism for each source is needed to lay the foundations of a better classification.

Most of the sources studied here are type I, of the kind apparently associated with regions of star formation; the earlier designation 'associated with HII regions' is not wholly appropriate since, with the advent of more accurate positions, precise agreement with individual HII regions is often not found, although the presence in the *general* vicinity of HII regions (recent star formation) is common. These sources are to be contrasted with the type I masers associated with the circumstellar shells surrounding late-type stars (e.g. the M giants and Mira variables). Some unique and hence unclassifiable sources include OH 284·18−0·79 and OH 231·8+4·2. The latest analysis of OH 284·18−0·79 (Allen, Hyland and Caswell, in preparation) suggests that it is a circumstellar object but with the spectral type of the star earlier (A2) than most such objects. The OH emission of OH 231·8+4·2 (also called 0739−14) is strongest at 1667 MHz and is very broad and unpolarized. Our survey would have been sensitive to further examples of either of these types of object, but none were found.

We also recall that two of the main-line masers in our survey, OH 327·40+0·45 and OH 337·00−0·02, may be associated with SNRs—a possibility meriting closer investigation since it is without precedent.

## 5. Conclusions

The sample of OH masers which we have detected constitutes a valuable search list for the following.

(1) *Possibly related HII regions or protostars.* Studies of radio continuum emission and IR emission should yield the proportion of OH masers existing in well-established regions of star formation (with extensive HII regions) and those in new regions of current star formation (with no readily detectable HII regions). These latter kinds (already crudely identified by our remarks on the lack of any continuum radio source nearby) may be especially useful in further studies of stars in the making.

(2) *Accompanying excited-state OH masers.* From past experience a relatively small fraction show detectable OH maser emission in the excited states but a renewed search of a large sample could yield valuable clues to the pumping mechanism.

(3) *Related $H_2O$ masers.* Some of this work has been carried out in parallel with the present survey (Batchelor *et al.* 1979). It is still a matter of dispute as to whether $H_2O$ masers form at an epoch in star formation significantly earlier than OH masers do. Surveys of masers of both species and the character of their surroundings should resolve this question.

As we pointed out in Section 4*a*, there is an urgent need to resolve the distance ambiguity for as many sources as possible. In those cases where HII regions are found to be associated we hope to achieve this by HI absorption measurements—as has been done for a small sample by Caswell *et al.* (1975). When this has been completed it will be possible to make an improved assessment of the number of galactic OH masers, which would then be a valuable parameter in the study of star formation in the Galaxy.

## References


Batchelor, R. A., Caswell, J. L., Goss, W. M., Haynes, R. F., Knowles, S. H., and Wellington, K. J. (1979). *Aust. J. Phys.* **33**, 139.

Bowers, P. F. (1978). *Astron. Astrophys.* **64**, 307.

Bowers, P. F., and Kerr, F. J. (1977). *Astron. Astrophys.* **57**, 115.

Caswell, J. L., and Haynes, R. F. (1975). *Mon. Not. R. Astron. Soc.* **173**, 649.

Caswell, J. L., Haynes, R. F., and Goss, W. M. (1977). *Mon. Not. R. Astron. Soc.* **181**, 427.

Caswell, J. L., and Lerche, I. (1979). *Mon. Not. R. Astron. Soc.* **187**, 201.

Caswell, J. L., Murray, J. D., Roger, R. S., Cole, D. J., and Cooke, D. J. (1975). *Astron. Astrophys.* **45**, 239.

Caswell, J. L., and Robinson, B. J. (1974). *Aust. J. Phys.* **27**, 597.

Clark, D. H., and Caswell, J. L. (1976). *Mon. Not. R. Astron. Soc.* **174**, 267.

Cook, A. H. (1975). *Mon. Not. R. Astron. Soc.* **171**, 605.

Davies, R. D., Booth, R. S., and Perbet, J.-N. (1977). *Mon. Not. R. Astron. Soc.* **181**, 83.

Elldér, J., Rönnäng, B., and Winnberg, A. (1969). *Nature* **222**, 67.

Genzel, R., and Downes, D. (1979). *Astron. Astrophys.* **72**, 234.

Goss, W. M., Manchester, R. N., and Robinson, B. J. (1970). *Aust. J. Phys.* **23**, 559.

Haynes, R. F., and Caswell, J. L. (1977). *Mon. Not. R. Astron. Soc.* **178**, 219.

Haynes, R. F., Caswell, J. L., and Simons, L. W. J. (1978). *Aust. J. Phys. Astrophys. Suppl.* No. 45.

Haynes, R. F., Caswell, J. L., and Simons, L. W. J. (1979*a*). *Aust. J. Phys. Astrophys. Suppl.* No. 48.

Haynes, R. F., Murdin, P. G., Thomas, R. M., Duldig, M. L., and Greenhill, J. G. (1979*b*). *Mon. Not. R. Astron. Soc.* **188**, 13.

Johansson, L. E. B., Anderson, C., Goss, W. M., and Winnberg, A. (1977). *Astron. Astrophys.* **54**, 323.

Knowles, S. H., Caswell, J. L., and Goss, W. M. (1976). *Mon. Not. R. Astron. Soc.* **175**, 537.

Robinson, B. J., Caswell, J. L., and Goss, W. M. (1974). *Aust. J. Phys.* **27**, 575.

Schmidt, M. (1965). *In* 'Galactic Structure' (Eds A. Blauuw and M. Schmidt), p. 513 (Univ. Chicago Press).

Sullivan, W. T., and Kerstholt, J. H. (1976). *Astron. Astrophys.* **51**, 427.

Turner, B. E. (1969). *Astrophys. J.* **157**, 103.

Wilson, T. L., Mezger, P. G., Gardner, F. F., and Milne, D. K. (1970). *Astron. Astrophys.* **6**, 364.


Manuscript received 10 August 1979, accepted 9 November 1979